Author's Response to Anonymous Referee 1

Anonymous Referee #1:

The study by Yu et al. investigates the impact of central (CP) and eastern (EP) Pacific El Niño events on the occurrence of winter haze days (WHD) in the JJJ region in northern China. Based on a statistical analysis of observational data and reanalysis products they conclude that EP El Niño increase the number of WHDs while CP El Niño events decrease their number. Variations in atmosphere circulation patterns over northern China during CP and EP events are suggested to cause this effect.

The manuscript is well structured and presents a thorough analysis on an interesting topic. The presented numbers, however, do not support the claim of a strong effect of the different types of El Niño events on WHDs in the JJJ region (see detailed comments below). I believe that the study is interesting enough to be published but that the conclusions must be formulated much more carefully and worded more in terms of tendencies. I summarise my concerns and list some specific comments below.

Reply: Thanks for the referee's positive comments and constructive suggestions. We have taken the referee's comments into consideration and carefully revised the manuscript. Please see our detailed point-by-point reply below.

Major concerns:

Q1: All correlations between the ENSO indices and WHDs as well as changes (e. g. in circulation types) related to ENSO events are very low.

a) Fig.1 displays pretty low correlations and I have a hard time to believe that they are actually statistically significant when averaged over the region (Table 2). How were the degrees of freedom determined for the student t-test? Even if statistically significant, such low correlation values don't argue for a strong impact of ENSO.

   Reply: We sampled the monthly data in each winter (December, January, and February) from 1961 to 2012, which means that the degree of freedom is 154. According to the threshold table of correlation coefficient (Zhou and Zheng, 1997), the absolute values of correlation coefficients between the site-averaged WHDs and EP and CP El Niño indices (Table 2) are larger than the threshold of 0.154. This indicates that they are statistically significant. Compared to the single site-observed WHDs, the correlations between the site-averaged WHDs and El Niño indices are easier to pass the significance test because the disturbances of local emissions, urbanization, and topography on WHDs may be eliminated. In addition, the correlation analysis is the primary step. We further elaborated the opposite impacts of two types El Niño events on the WHD in the JJJ region via exhibiting the differences between the changes in WHDs in two type El Niño years (Figures 2 and 3).

   We agree with you that the low correlation values may not argue for a strong impact of ENSO. We have supplemented such description. Please see Lines 156-157 and 311-313 in the revised manuscript.

   References:

   Zhou, Y. H. and Zheng, D. W.: A new calculation method of correlation coefficient test table. Annals of Shanghai Observatory Academia Sinica, 18, 18-23, 1997.

b) The response to CP El Niño events to be more consistent (judging from the composite change shown in Fig. 2) but the response to EP El Niño events looks rather variable from station to station (Fig. 1 and 2).

Reply: Haze pollution is a sophisticated problem because it includes the comprehensive impacts of emissions, weather conditions, and even topography. This may lead to some biases of correlation coefficients among different sites when examining the correlations between the single-site WHDs and El Niño indices. But we can still find the consistently composite positive WHD anomalies, corresponding to EP El Niño years, at most sites (149 sites; accounting for 76.4% of all sites) in the JJJ region in Fig. 2b. In addition, the positive correlation between EP El Niño events and WHDs is also illustrated at 121 stations (accounting for 62.1% of all stations; Fig. 1b). The corresponding proportion will increase to 70.5% if we only consider the stations at which the correlations pass a significance level of 90%. We have supplemented quantitative descriptions to highlight the positive correlations between the WHDs and EP El Niño events. Please see Lines 147-154 and 161-164 in the revised manuscript.

c) The box-and-whisker plot (Fig. 3a) indicates that there is quite some spread in the response between individual EP and CP events.

Reply: The aerosol pollutants in the JJJ region are not only subject to the interannual change of emissions and the multiple-time scale climate changes as we discussed in the section 4, but also affected by the variations in local emissions, urbanization, and topography. These result in differences in distributions of WHD anomalies among individual EP and CP El Niño years and some spread of WHD anomalies in special El Niño year. However, we do find out the variations of WHD anomalies in phase with individual EP and CP El Niño years (Fig. 3a), which are characterized by a larger distribution in the positive range in response to most of EP El Niño years, but a larger distribution in the negative range in response to most of CP El Niño years. The site-averaged results also indicate the opposite distribution of changes in WHD corresponding to EP and CP El Niño years (Fig. 3b). We have supplemented more explanation about the box-and-whisker plot to elaborate our results. Please see Lines 171-173 in the revised manuscript.

d) From the numbers on the change in circulation types (Table 3 and corresponding text), I would actually conclude that there is hardly any effect of El Niño but maybe I am missing something here?

Reply: Indeed. These composite changes in the occurrence frequency of both pollution and clean circulation types seem to be small corresponding to EP and CP El Niño years. However, it is more complicated when we examine those changes for each circulation type. For example, in the winter of EP El Niño years, the changes in the occurrence frequency of the pollution (clean) circulation types range from -0.53% (-0.95%) to 1.97% (0.45%). The corresponding changes range from -2.33% (-0.4%) to 1.55% (0.84%) in the winter of CP El Niño years. The values may be small when calculating the composite changes. In addition, it is more difficult to further link the changes in WHDs to variation of a specific circulation type due to the lack of long-term daily haze pollution data. But we can generally explain the WHD anomalies in EP and CP El Niño years according to the composite changes in occurrence frequency of both pollution and clean circulation types. Finally, there is no formula currently to quantitatively describe the relationship between synoptic-scale circulation anomalies and haze pollution. More detailed works are needed in the future. We have supplemented more details in Table 3 and corresponding text. Please see Lines 268-277 in the revised manuscript.

Q2: It is stated that the number of haze days changes roughly by 2 during El Niño events (Fig. 2 and corresponding text). How does that compare to the average number of haze days?

Reply: The changes of 2 haze days account for 17% to 79% and -13% to -70% of the average numbers of haze days, respectively, at these sites. We have added the figure of percentages of WHD anomalies in all El Niño, EP El Niño, and CP El Niño years, respectively, relative to the climatological means (new Figure S2). We have also supplemented some descriptions in the revised manuscript. Please see Lines 161-164 in the revised manuscript.

Q3: Regarding the eight circulation types identified in section 3.3 I find it very hard to see the difference between some of them. What determines the number of these types? Since they are grouped together in the following anyway, is it necessary to distinguish between all of them?

Reply: We have supplemented the difference in each circulation type in Table 3. In this study, we used the K-means clustering algorithm to classify different circulation types. The optimal number of classifications is determined by the inflection point of criterion function. More detail descriptions are reported in Liu and Gao (2011). There remain some differences in the patterns of circulation anomalies among different pollution or clean circulation types in Figures 5, 6 and 7, although their common variations can be used to explain the WHD anomalies in response to EP and CP El Niño years. The differences may further relate to the intraseasonal changes in haze pollution. However, as answered in Q1 (d), exploring this link needs long-term daily haze pollution data, which is lacking at present.

References:

Liu, D. and Gao, S. C.: Determining the number of clusters in K-means clustering algorithm. Silicon Valley, 6: 38-39, 2011.

Specific comments:

Q4: line 9: The first sentence of the abstract sounds strange to me. Maybe use “The El Niño-Southern Oscillation” instead of just “El Niño”.

Reply: We have changed this sentence into “El Niño is complicated due to its diverse distribution features and intensities.”. Please see Line 9 in the revised manuscript.

In this study, we only focus on the impacts of El Niño, but not the La Niña. Therefore, it may be more accurate to only mention "El Niño" here.

Q5: line 53: What is meant by “Integral El Niño events”?

Reply: The "Integral El Niño events" used here means the overall El Niño events without classification. We have revised it. Please see Line 53 in the revised manuscript.

Q6: line 55 to 57: EP and CP El Niño are different flavours of the same climate mode

Reply: It may be an ambiguity here. We agree with you that both types of El Niño events are the warm conditions of El Niño–Southern Oscillation—the leading climate mode of interannual variability in the tropical Pacific. However, we want to emphasize two dynamic modes of quasi-quadrennial and quasi-biennial oscillations at here. These independent modes coexist in the tropical Pacific and may modulate the features of ENSO due to their interannual and interdecadal changes (Bejarano et al., 2008; Wang and Ren, 2017). Their interplay also contributes to the spatial diversity of the observed ENSO events, like EP and CP El Niño (Timmermann et al., 2018). We have revised the manuscript to avoid the ambiguous expression. Please see Lines 55-59 in the revised manuscript.

References:

Bejarano, L. and Jin, F. F.: Coexistence of equatorial coupled modes of ENSO. Journal of Climate, 21(12): 3051-3067, doi:10.1175/2007jcli1679.1, 2008.

Timmermann, A., An, S. I., Kug, J. S., Jin, F. F., Cai, W. J., Capotondi, A., Cobb, K., Lengaigne, M., McPhaden, M. J., Stuecker, M. F., Stein, K., Wittenberg, A. T., Yun, K. S., Bayr, T., Chen, H. C., Chikamoto, Y., Dewitte, B., Dommenget, D., Grothe, P., Guilyardi, E., Ham, Y. G., Hayashi, M., Ineson, S., Kang, D., Kim, S., Kim, W. M., Lee, J. L., Li, T., Luo, J. J., McGregor, S., Planton, Y., Power, S., Rashid, H., Ren, H. L., Santoso, A., Takahashi, K., Todd, A., Wang, G. M., Wang, G. J., Xie, R. H., Yang, W. H., Yeh, S. W., Yoon, J., Zeller, E., and Zhang, X. B.: El Niño–Southern Oscillation complexity. Nature,

559(7715): 535-545, doi:10.1038/s41586-018-0252-6, 2018.
Wang, R. and Ren, H. L.: The linkage between two ENSO types/modes and the interdecadal changes of ENSO around the year 2000. Atmospheric and Oceanic Science Letters, 10(2): 168-174, doi:10.1080/16742834.2016.1258952, 2017.

Q7: line 71 to 73: Does this classification differ from other commonly used ENSO classifications?

Reply: Yes, it does. This classification is based on an equation set that contain two ENSO indexes (Niño 3 and Niño 4 index) as shown in section 2.2, although it still employs the common monitoring areas of sea surface temperature anomalies. At present, there are quite some differences among the monitoring results for the same ENSO event due to employ differently single index, like the Japan Meteorological Agency (JMA) index, the Multivariate ENSO Index (MEI), and the El Niño Modoki Index (EMI). The classification used in this study shows the better performance in monitoring different types of historical ENSO events and determining the characteristics of the ENSO events than any single index. This has been reported in previous studies (Cao et al., 2013; Ren et al., 2017).

References:

Cao, L., Sun, C. H., Ren, F. M., Yuan, Y. and Jiang, J.: STUDY OF A COMPERHENSIVE MONITORING INDEX FOR TWO TYPES OF ENSO EVENTS. Journal of Tropical Meteorology, 29(1):66-74, 10.3969/j.issn.1004-4965.2013.01.008, 2013.
Ren, H. L., Sun, C. H., Ren, F. M., Yuan, Y., Lu, B., Tian, B., Zuo, J. Q., Liu, Y., Cao, L, Han, R. Q., Jia, X. L. and Liu, C. Z.: Identification method for El Niño/La Niña events. The People's Republic China's National Standard GB/T 33666-2017, May 2017. Beijing: Standards Press of China, 1-6, 2017.

Q8: line 150-152: Obviously the averaged correlation values are higher if only values above a certain threshold are considered. I am not sure what to learn from that.

Reply: As mentioned in Q1, the variations in local emissions, urbanization, and topography make haze pollution in the JJJ region more complicated. These factors not only lead to some biases of correlation coefficients among different sites when examining the correlations between the single-site WHDs and El Niño indices, but also contribute to the lower correlations between the site-averaged WHD and El Niño indices. Therefore, we selected the stations at which the correlations pass a significance level of 90% and calculated the correlations between different El Niño indices and the averaged WHDs at these stations. These higher correlation coefficients of 0.31 and -0.43, corresponding to EP and CP El Niño events, further illustrate the significant opposite impacts of two types El Niño on the WHDs in the JJJ region.

Q9: line 190: "worsening meteorological conditions": worse in what respect and compared to what?

Reply: As reported in the previous studies (Chen et al., 2015; Chang et al., 2016), the lower sea surface pressure and the higher surface air temperature in the northeastern Eurasia are favorable for the maintenance and development of atmospheric pollutant and defined as the worsening meteorological conditions (Zhang et al., 2018). In this study, the above anomalies are apparent in the winter of EP El Niño years.

References:

Chang, L. Y., Xu, J. M., Tie, X. X., and Wu, J. B.: Impact of the 2015 El Nino event on winter air quality in China. Scientific Reports, 6(1):34275, doi:10.1038/srep34275, 2016.
Chen, H. P. and Wang, H. J.: Haze Days in North China and the associated atmospheric circulations based on daily visibility data from 1960 to 2012. Journal of Geophysical Research Atmospheres, 120(12):5895-5909, doi:10.1002/2015jd023225, 2015.
Zhang, X. Y., Zhong, J. T., Wang, J. Z., Wang, Y. Q., and Liu, Y. J.: The interdecadal worsening of weather conditions affecting aerosol pollution in the Beijing area in relation to climate warming. Atmospheric Chemistry and Physics, 18(8),

5991-5999, doi:10.5194/acp-18-5991-2018, 2018.

Q10 line 312: “greatly worth concern” Please rephrase.

Reply: We have changed the description here into “The impacts of worsening meteorological conditions caused by annual climate change on the haze pollution process are worthy of concern.”. Please see the Lines 343-344 in the revised manuscript.

Author's Response to Anonymous Referee 2

Anonymous Referee #2:

Review comments for "Contrasting impacts of two types of El Niño events to winter haze days in China's Jing-Jin-Ji region" by Yu et al., (2020).

In this study, the authors tele-linked the El Niño events and wintertime haze pollution in Northern China. This study concludes that the occurrence of pollution is connected with El Niño modes. Generally speaking, the paper can be significantly improved with the inclusion of chemical research and discussion when dealing with the haze topic (e.g., the composition and response by each species). This study is more like a purely statistical analysis with insufficient mechanism explanations. Moreover, the overall structure of this paper is somewhat mixed up and the English of this study needs some improvements. I have the following concerns before the formal publication of this study.

Reply: Thank you very much for the thorough comments and suggestions. These comments and suggestions are very helpful to improve the quality of the manuscript. We have made revisions according to these comments. Please find the following point-point reply. In addition, the English of the manuscript has been improved by native speakers of English. For a certificate, please see: http://www.textcheck.com/certificate/fUwXLd

Specific concerns:

Q1: This study emphasized haze days, however, without specifying the source of haze. For example, the chemistry here should definitely be discussed. Is PM the one to blame? If so, what is the composition? Also, when conducting the correlation analyses, what are the correlation to individual particle types? Any size distribution biases?

Reply: Thanks a lot for these helpful comments. We agree with you that anomalous weather conditions may affect the chemistry of some aerosol types, such as sulfate and nitrate. However, the haze days defined by visibility and relative humidity is the only available long-term observation data that reflects air pollution levels in China. There are few long-term large-scale observations of aerosol composition, particle types, and size distribution in China for the correlation analyses. More detailed analyses need to be solved by gathering more observations and performing some sensitive simulations in future work. Alternatively, we added more analyses and discussions to further illustrate that the variations of WHDs in the JJJ region in response to EP and CP El Niño years are more attributed to the regional transport of aerosol pollutants caused by two types of El Niño. Please see the last paragraph of both section 3.2 and section 4 in the revised manuscript.

Q2: In this study, the Niño data used were provided by CMA. I am wondering what is the difference between the CMA Nino data and NOAA nino data? Authors should give more in-depth descriptions on the products they use.

Reply: The definitions of the Niño indices between CMA and NOAA are the same. Referring to the People's Republic China's National Standard (Ren et al., 2017), the Niño indices provided by CMA are calculated using the Hadley Centre Sea Ice and Sea Surface Temperature Data (HadISST) from March 1961 to December 1981 and the National Oceanic and Atmospheric Administration (NOAA) daily optimum interpolation (OI.v2) SST dataset from January 1982 to February 2013. We have supplemented these descriptions. Please see Lines 89-92 in the revised section 2.1.

References:

Ren, H. L., Sun, C. H., Ren, F. M., Yuan, Y., Lu, B., Tian, B., Zuo, J. Q., Liu, Y., Cao, L, Han, R. Q., Jia, X. L. and Liu, C. Z.: Identification method for El Niño/La Niña events. The People's Republic China's National Standard GB/T 33666-2017,

Q3: The authors heavily relied on the ERA data for both ERA-40 and ERA-interim. Why not using the latest ERA5 data instead? I understand the ERA-40 is for older records but the ERA5 should be available for more recent years. Using state-of-art products boost the innovative part of this study.

Reply: Thanks a lot for this advice! We have reexamined our results using the latest ERA5 data and compared them with our original results. In the new results, the data from March 1961 to December 1978 are derived from the ERA-40 reanalysis data and that from January 1979 to February 2020 are derived from the ERA5 reanalysis data. As seen in Figures A1a and e, there are increases in surface air temperature (SAT) over northern China in the winters of EP El Niño years, but corresponding decreases in the winters of CP El Niño years, which are more obvious than our original results. Similar to Figures A1a and e, the opposite patterns of sea level pressure (SLP) anomalies over northern China in response to two types of El Niño years are shown in Figures A1b and f, although these anomalies are weaker than our original results. The patterns of geopotential height anomalies at 500 hPa corresponding to the EP and CP El Niño years are generally consistent with our original results. But the resulting changes in wind over northern China in the winter of both EP and CP El Niño years are weaker for the new data. For the changes in intraseasonal atmospheric circulation in each circulation type in response to two types of El Niño years, there are some differences between the new and original results (Figures A2, 3, and 4). However, the new results still capture the decreased SLP gradients, the southerly wind and positive SAT anomalies in most of circulation types in the winters of EP El Niño years over the JJJ region (Figures A2, A4a and e). Meanwhile, the opposite anomalies, such as increased SLP gradients, northerly wind, and negative SAT anomalies, corresponding to the CP El Niño years are shown in the new results (Figures A3, A4b and d). In brief, the new results also clearly show the differences of atmospheric circulations corresponding to two types of El Niño years at both interannual and interdecadal timescales. These are in line with our original analyses, so we didn't replace the data in this manuscript.

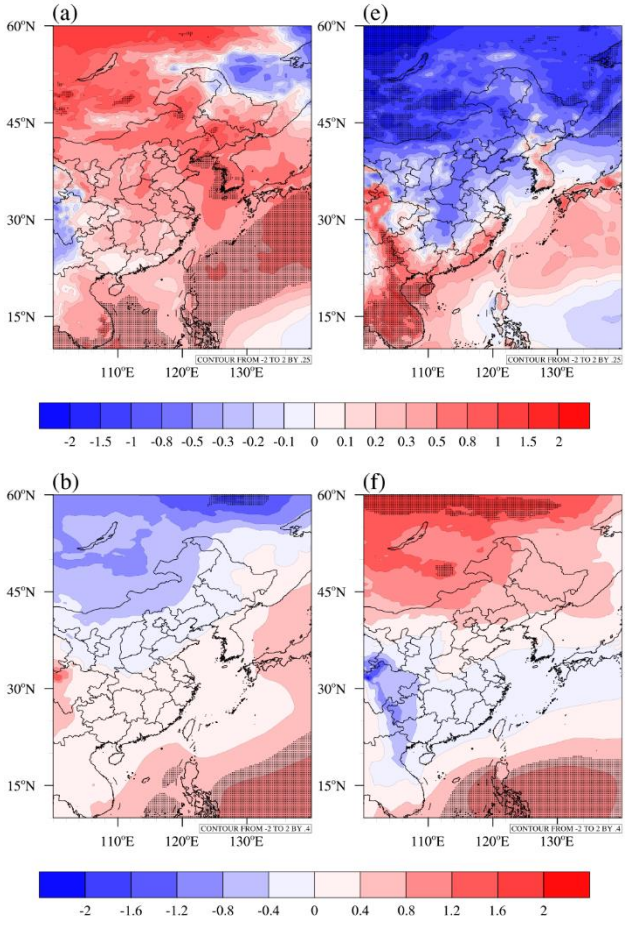

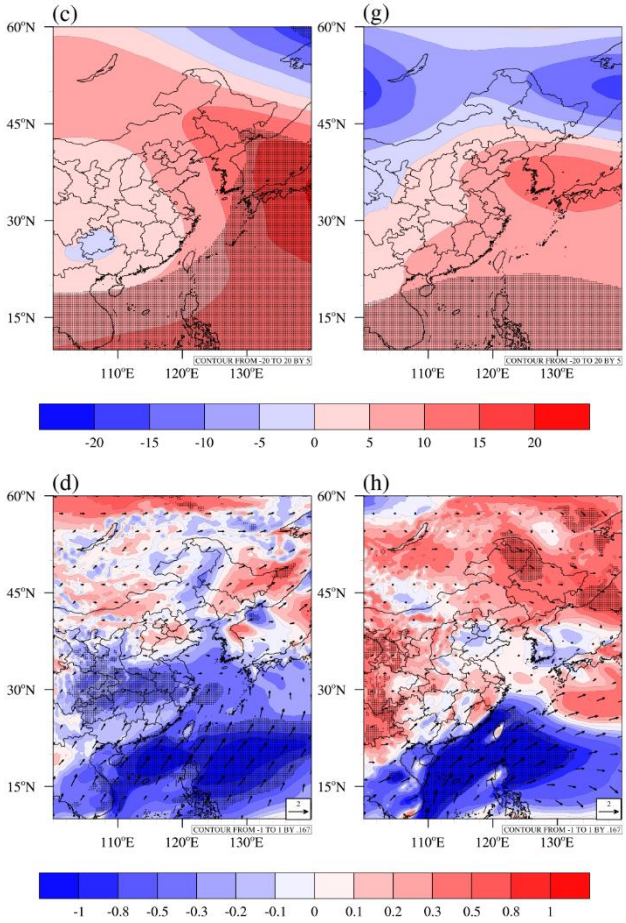

Figure A1: Winter mean changes in (a, e) air temperature at 2 meter (unit: K), (b, f) sea level pressure (unit: hPa), (c, g) geopotential height at 500 hPa (unit: gpm), and (d, h) wind averaged from 1000 hPa to 850 hPa (The arrows represent wind vectors and the contours represent wind velocities, unit: m s^{-1}) in responses to the two types of El Niño. The left (a-d) and right (e-h) panels represent the differences averaged in 11 EP El Niño and 7 CP El Niño years, respectively, relative to the 1961-2020 climatological means. The dots indicate significance at ≥ 90% confidence level from the t test.

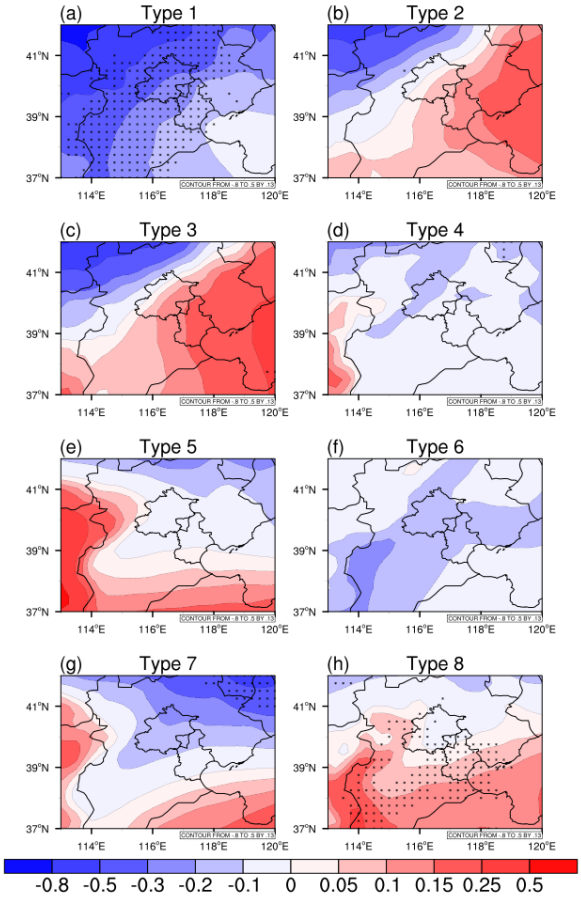

Figure A2: Same as Figure 5, but using the new data set.

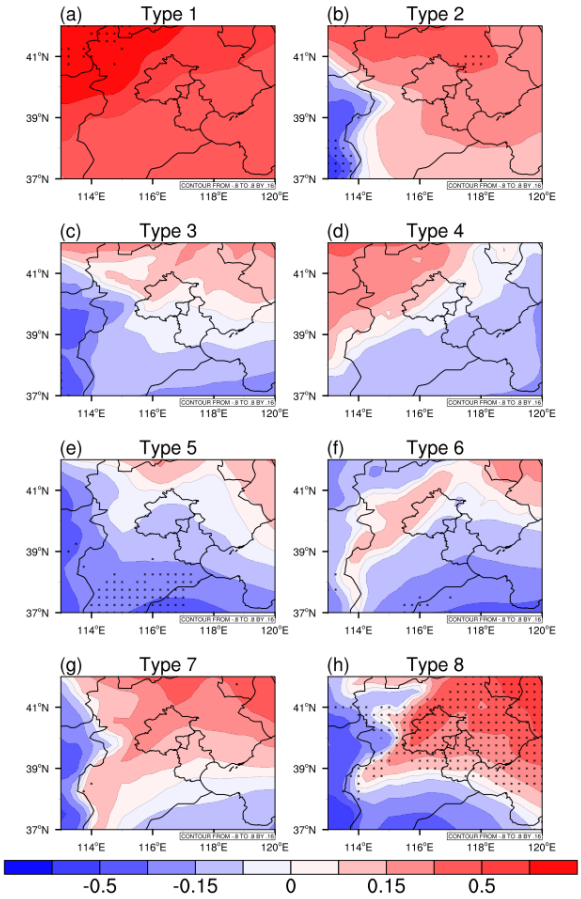

Figure A3: Same as Figure 6, but using the new data set.

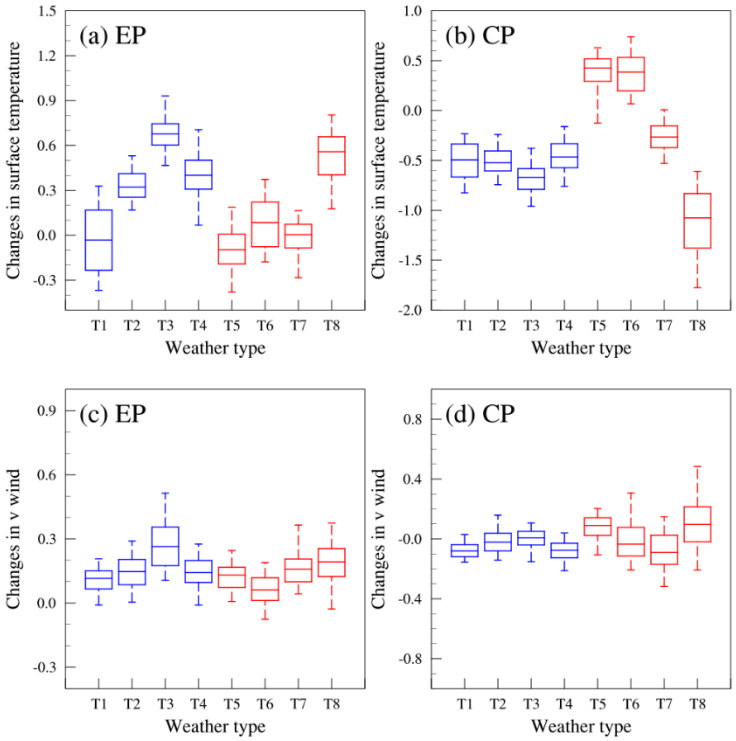

Figure A4: Same as Figure 7, but using the new data set.

Q4: The authors should expand section 2.3. The described method was very generic and details-lacking. It is very hard for readers to comprehend what has been done. Also, the first two paragraphs of 3.1 should be placed in the method section instead of the results.

Reply: Accepted. We have revised the section 2.3 to make sure that readers can clearly understand what has been done. In addition, we have moved the first paragraph of section 3.1 to section 2 as a separate section 2.4. The second paragraph of section 3.1 includes more results of correlation analysis, so we remain it in the original section. Please see the revised section 2.3, 2.4, and 3.1.

Q5: It is hard to tell whether the correlation results shown in Figure 1 are significant or not as the highest correlation is around 0.5 for both positive and negative correlations. Can authors please justify the significance of these correlation numbers?

Reply: All the correlation results shown in Figure 1 are significant at 90% confidence level. We have revised the figure caption. Please see the revised manuscript.

Q6: The caption of Figure 5 “The dots indicate that the differences between more than 60

Reply: We guess that the referee wants to know more details about the dots. We sampled daily data corresponding to each of synoptic-scale circulation types in 10 EP El Niño years, and then calculated the differences by subtracting the 1961-2013 climatological averaged result of each types from them. The dots indicate that more than 60% of all the differences have the same sign as the mean differences. This approach to some extent represents the statistics significance of the results.

Q7: Since this paper primarily focuses on the JJJ region, I would recommend authors to highlight the boundary of this region when making the plots, especially in zoomed-in cases (e.g., Figures 1, 2 and 5).

Reply: We agree entirely with the referee’s view. We have highlighted our research domain of the JJJ region with the green boxes in Figures 1, 2 and S2. Note that the areas shown in Figures 5 and 6 are entirely consistent with our research domain.

Q8: Authors, please check the right panel of Figure 3 for CP_{year}. The lower whisky overlap with 25.

Reply: Thank you for your reminding. We have replaced the winter mean data with three monthly data sampled from each El Niño winter and replotted this figure. In addition, we have also replaced the extremums with the 5th and 95th percentile. Please see the revised manuscript.

Q9: This paper discusses the positive precipitation anomaly for the CP case. How about the precipitation for the EP case?

Reply: As seen in Figure 4e, the monthly precipitation is generally increased over southern China in the winters of EP El Niño years, with the maximum changes exceeding 10 mm. But there are slightly negative anomalies of precipitation over central and northeastern China. The area with positive precipitation anomalies over the JJJ region is smaller in EP El Niño years compared to that in CP El Niño years, although a comparable increase in precipitation over this region occurs with both types of El Niño years. We have increased the description of precipitation anomalies in response to EP El Niño years. Please see Lines 225-226 in the revised manuscript.

Q10: In Figure 1, I noticed one dot has distinctive signs between nino 3.4 and EP, shown below in square. Why is that case? I assume these two regions shall be pretty close.

Reply: Two stations with close distance may belong to urban and rural areas, respectively. This can lead to a distinct difference in their underlying surface and local emissions. In addition, two stations with close distance may differ greatly in altitude due to the complicated terrain. The above factors will complicate haze pollution and may be the reason for the distinctive difference in signs between two adjacent stations.

A list of all relevant changes made in the manuscript in response to Referee 1

Changes made in the manuscript	Corresponding questions
Line 9 in Abstract	Q4
Line 53 in section 1	Q5
Lines 55-59 in section 1	Q6
Lines 147-154, 156-157, 161-164, and 171-173 in section 3.1	Q1(a), (b), (c), and Q2
Lines 268-277 in section 3.3	Q1(d)
Lines 311-313 in section 4	Q1(a)
Lines 343-344 in section 4	Q10
Table 3	Q1(d) and 3

A list of all relevant changes made in the manuscript in response to Referee 2

Changes made in the manuscript	Corresponding questions
Lines 89-92	Q2
Section 2.3, 2.4, and 3.1	Q4
Line 164-167 in section 3.1	Language improvements
Lines 225-226 in section 3.2	Q9
Last paragraph of section 3.2	Q1
Last paragraph of section 4	Q1
Reference	Q1
Figure 1	Q5 and 7
Figure 2	Q7
Figures 3 and 7	Q8

Contrasting impacts of two types of El Niño events on winter haze days in China's Jing-Jin-Ji region

Xiaochao Yu[1,2], Zhili Wang[1*], Hua Zhang[1], Jianjun He[1], Ying Li[3]

[1]State Key Laboratory of Severe Weather and Key Laboratory of Atmospheric Chemistry of CMA, Chinese Academy of Meteorological Sciences, Beijing, 100081, China

[2]Department of Atmospheric and Oceanic Sciences, Fudan University, Shanghai, 200438, China.

[3]National Climate Center, China Meteorological Administration, Beijing, 100081, China

Correspondence to: Zhili Wang (wangzl@cma.gov.cn)

Abstract. El Niño is complicated due to its diverse distribution features and intensities. The regional climate anomalies caused by different types of El Niño event likely lead to various impacts on winter haze pollution in China. Based on long-term site observations of haze days in China from 1961 to 2013, this study explores the effects of Eastern Pacific (EP) and Central Pacific (CP) types of El Niño events on the number of winter haze days (WHD) in China's Jing-Jin-Ji (JJJ) region and the physical mechanisms underlying WHD changes. The results show statistically significant positive and negative correlations, respectively, between WHD in the JJJ region and EP and CP El Niño events. At most sites in the JJJ region, the average WHD increased in all EP El Niño years, with the maximum change exceeding 2.0 days. Meanwhile the average WHD decreased at almost all stations over this region in all CP El Niño years, with the largest change being more than -2.0 days. The changes in large-scale circulations indicate obviously positive surface air temperature (SAT) anomalies and negative sea level pressure (SLP) anomalies over North China, and southerly wind anomalies at the mid-low troposphere over eastern China in the winters of EP El Niño years. These anomalies are conducive to increases in WHD in the JJJ region. However, there are significant northerly and northwesterly wind anomalies at the mid-low troposphere over eastern China, and stronger and wider precipitation anomalies in the winters of CP El Niño years, which contribute to decreased WHD over the JJJ region. Changes in local synoptic conditions indicate negative SLP anomalies, positive SAT anomalies, and weakened northerly winds over the JJJ region in the winters of EP El Niño years. The total occurrence frequency of circulation types conducive to the accumulation (diffusion) of aerosol pollutants is increased (decreased) by 0.4% (0.2%) in those winters. However, the corresponding frequency is decreased (increased) by 0.5% (0.6%) in the winters of CP El Niño years. Our study highlights the importance of distinguishing the impacts of these two types of El Niño events on winter haze pollution in China's JJJ region.

1 Introduction

North China, with the Jing-Jin-Ji (JJJ) region at the core, has encountered continuous severe haze pollution in recent winters. These atmospheric calamities have seriously harmed traffic, economic development, and resident health in this region (Gao et al., 2017; Liu et al., 2017; Zhang et al., 2019a). Increased anthropogenic emissions are considered the predominant reason for the increased frequency and intensity of haze pollution. However, many studies have verified the effects of worsening local weather conditions caused by large-scale climatic anomalies on severe haze events (Li et al., 2016; Cai et al., 2017; Li et al., 2018; Yin and Wang, 2018). Anomalous meteorological conditions have significant influences on the development and maintenance of haze events; in particular, the explosive increase in local air pollutants is always accompanied by anomalous atmospheric circulation conditions (He et al., 2018; Zhang et al., 2018; Zhong et al., 2018). Hence, identifying the mechanism underlying the response of haze events to worsening weather conditions caused by interannual climate changes has implications for effectively controlling haze pollution and improving air quality.

As a strongest signal of interannual climate variation (Wyrtki, 1975; Cane, 2005), El Niño has an important influence on the maintenance and diffusion of air pollutants via affecting large-scale atmospheric circulation and precipitation (Feng et al., 2016a, 2016b; Zhao et al., 2018), and consequently modulates the interannual variation of winter haze days (WHD) in China (Gao and Li, 2015; Sun et al., 2018; He et al., 2019). Several studies have reported that an anomalous anticyclone develops over the Northwest Pacific during the maturation of El Niño, resulting in increased precipitation and decreased WHD in southern China (Li et al., 2017; Zhao et al., 2018; He et al., 2019). Moreover, atmospheric circulation anomalies caused by El Niño can exacerbate the northward transport of aerosols in South and Southeast Asia, thereby increasing winter mean aerosol concentrations (Feng et al., 2016a) and intraseasonal severe haze days in eastern China (Zhao et al., 2018; Yu et al., 2019). Recent studies have indicated that there is a significant negative correlation between El Niño and WHD in southern China (Li et al., 2017; Zhao et al., 2018; He et al., 2019). However, the impacts of El Niño on WHD in northern China remain controversial. For example, Sun et al. (2018) showed that El Niño led to increased WHD in North China by suppressing the activity of the East Asian winter monsoon (EAWM). However, based on statistical analyses of long-term site observations of WHD in China, several studies have found no statistically significant correlation between El Niño indices and WHD in North China (Li et al., 2017; Zhao et al., 2018; He et al., 2019).

The above studies mostly focused on analyzing the comprehensive impacts of all El Niño events on WHD in China. Their results indicated that the effect of El Niño events on air pollutants in northern China was much weaker than that in southern China (Li et al., 2017; Zhao et al., 2018; He et al., 2019). However, the El Niño-Southern Oscillation (ENSO) is a complex system with two dominant modes of quasi-quadrennial and quasi-biennial oscillations coexisting in the tropical Pacific (Bejarano et al., 2008; Wang and Ren, 2017). Its warm conditions (El Niño) can be classified into the Eastern Pacific (EP) and Central Pacific (CP) El Niño according to the anomalous sea surface temperature (SST) patterns contributed by the interplay of these independent modes (Ashok et al., 2007; Levine et al., 2010; Roberts et al., 2016; Timmermann et al., 2018). Because of the significantly distinct SST anomaly patterns in the equatorial Pacific, the two types of El Niño events have different influences on the Walker circulation, which further stimulates global circulation wave trains and results in contrasting temperature and precipitation anomalies in East Asia (Larkin et al., 2005; Yuan et al., 2012; Cai et al., 2018). The anomalies in regional climate caused by the two types of El Niño events may have different influences on winter atmospheric pollutants in China. For example, using the tropospheric chemical model GEOS-Chem, Feng et al. (2016a) showed that CP El Niño played an important role in redistributing seasonal mean $PM_{2.5}$ (particulate matter with a diameter $\leq$ 2.5 μm) concentrations in China. Recently, Yu et al. (2019) also found significant opposite changes in winter mean aerosol concentrations and severe haze days in North China in the responses to different types of El Niño events by using a global aerosol-climate model. Nevertheless, the observation-based studies on the effects of the two types of El Niño events on haze pollutants in China are still insufficient. The JJJ region is one of the most densely populated areas in China and a typical region of severe air pollution (Cai et al., 2017; Miao et al., 2017; Zhong et al., 2018). Therefore, it is important to understand the different responses of WHD in this region to the two types of El Niño events in greater depth.

This study first classifies different types of El Niño events according to the latest national standard of the People's Republic of China (PRC) "Identification method for El Niño/La Niña events" issued by the China Meteorological Administration (CMA) (Ren et al., 2017). Then, we explore the impacts of the two types of El Niño events on WHD in China's JJJ region (37–42°N, 113–120°E) from the perspectives of large-scale circulation and local synoptic condition anomalies using long-term site observations and reanalysis datasets, combined with commonly used circulation type classification methods. The datasets and methods used in this study are presented in Section 2. The impacts of the two types of El Niño events on WHD in China's JJJ region and the potential physical mechanisms are analyzed in Section 3. The discussion and conclusions are presented in Section 4.

2 Methodology

2.1 Data

The datasets used in this study were as follows. (1) The monthly haze days dataset from the National Meteorological Information Center of the CMA. The time span of the dataset is from March 1961 to February 2013. According to a comprehensive judgment method widely used in previous studies, a haze day is identified when the daily mean visibility is less than 10 km and the daily mean relative humidity is less than 90% (Schichtel et al., 2001; Doyle et al., 2002; Wu et al., 2010). (2) The monthly Niño3 index (SST anomaly averaged over the Niño3 domain [150°W–90°W, 5°S–5°N]; $I_{Niño3}$), Niño4 index (same as the Niño3 index, but over the Niño4 domain [160°E–150°W, 5°S–5°N]; $I_{Niño4}$), and Niño3.4 index (same as the Niño3 index, but over the Niño3.4 domain [170°W–120°W, 5°S–5°N]; $I_{Niño3.4}$) from March 1961 to February 2013, provided by the National Climate Center of the CMA. All Niño indices are calculated using the Hadley Centre Sea Ice and Sea Surface Temperature Data (HadISST) from March 1961 to December 1981 and the National Oceanic and Atmospheric Administration (NOAA) daily optimum interpolation (OI.v2) SST dataset from January 1982 to February 2013 (Ren et al., 2017). (3) Daily and monthly ERA-40 and ERA-Interim reanalysis data from the European Centre for Medium-range Weather Forecasts (ECMWF), including sea level pressure (SLP), air temperature at 2 m, wind at 10 m, geopotential height at 500 hPa, and wind from 1000 to 850 hPa (composed of seven pressure levels at 850, 875, 900, 925, 950, 975, and 1000 hPa). The horizontal resolution is 0.25°×0.25°, and the time span is from March 1961 to February 2013 for both daily and monthly reanalysis data. The data from March 1961 to December 1978 are derived from the ERA-40 reanalysis data, and the data from January 1979 to February 2013 are derived from the ERA-Interim reanalysis data. (4) The global land surface precipitation data were provided by the Global Precipitation Climatology Centre (GPCC), with a horizontal resolution of 0.5°×0.5°, covering March 1961 to February 2013 (Schneider et al., 2014).

2.2 Identification of two types of El Niño events and calculation of their indices

Similar to Yu et al. (2019), we classified different types of El Niño events referring to the national standard of the PRC mentioned in Section 1. This method identifies El Niño events based on the widely used $I_{Niño3.4}$ and employs $I_{Niño3}$ and $I_{Niño4}$ to distinguish the different characteristics of the two types of El Niño events. $I_{Niño3}$ and $I_{Niño4}$ are highly sensitive to EP and CP El Niño events, respectively. This identification method has been applied to the climate operations of the CMA and has been widely used in research on the effects of El Niño events (e.g., Mu et al., 2017; Yu et al., 2019). We first selected all El Niño events from 1961 to 2013. An El Niño event is identified when the absolute value of the 3-month smoothing average of $I_{Niño3.4}$ reaches or exceeds 0.5°C for at least 5 months. All El Niño events were classified referring to the EP El Niño index (Iep) and the CP El Niño index (Icp). Iep and Icp were calculated as follows:

$$Iep = I_{Niño3} - (\alpha \times I_{Niño4}), \quad (1)$$

$$Icp = I_{Niño4} - (\alpha \times I_{Niño3}). \quad (2)$$

According to an empirical formula, the constant α is 0.4 if $I_{Niño3} \times I_{Niño4} > 0$, but 0 if $I_{Niño3} \times I_{Niño4} \leq 0$. An event is defined as an EP (CP) El Niño event if the absolute value of Iep (Icp) reaches or exceeds 0.5°C for at least 3 months. Table 1 shows the specific classifications of the two types of El Niño events obtained by the above method.

2.3 Circulation type classification methods

An aim of using circulation type classification is to identify the most frequently occurring subset of the meteorological data, thereby considering the numerous interrelated meteorological variables within an integrated framework and exploring the physical mechanisms underlying aerosol pollution in the JJJ region in the classification process (Richman et al., 1981; Miao et al., 2017). Among the multitudinous circulation classification techniques, the T-mode principal component analysis (PCA) combined with the K-mean cluster used in this study is the most effective identification approach because of its reproduction

of predefined types, temporal and spatial stability, and low dependence on preset parameters (Huth et al., 1996; Zhang et al., 2012). This method has been widely used to identify the circulation types associated with air pollution (He et al., 2017a, 2017b, 2018). Similar to He et al. (2018), daily SLP data from March 1961 to February 2013 in the JJJ region were taken as the samples for circulation type classification. First, we reshaped three-dimensional daily SLP data, including time, latitude, and longitude, into two-dimensional data (time × grid) and normalized the two-dimensional data for time series. Second, the normalized SLP data performed the T-mode PCA and its main components were obtained according to the cumulative variance contributions, up to a total of 95%. Third, we clustered the main components using the K-means cluster and identified the optimal number of clusters referring to the criterion function (Liu and Gao, 2011). In this study, the inflection point of the criterion function, which represents the optimal number of clusters, was eight. The daily SLP data were assigned to eight synoptic-scale circulation types based on the clustering result. The other variables (e.g., temperature at 2 m and wind at 10 m) were classified in the same way. Finally, each pattern of synoptic-scale circulation was determined.

2.4 Correlation analysis

The correlation coefficients of site-observed WHD in eastern China (east of 110°E) with the different types of El Niño indices (i.e., $I_{Nino3.4}$, Iep, and Icp) were calculated in this study. The sites without WHD for at least 25 consecutive years were eliminated before the correlation analysis, as the time series of WHD at these sites lack interannual and interdecadal fluctuations, and their responses to anomalous synoptic conditions caused by climate change are weak. In addition, a band-pass filtering of 2–10 years was performed for the WHD data to remove signal interference from changes in local aerosol emissions and interdecadal climate variability following Zhao et al. (2018) and He et al. (2019). The final results more intuitively reflect the correlation between El Niño events and WHD.

3 Results

3.1 Impacts of the two types of El Niño events on WHD in China's JJJ region

Figure S1 shows the correlation coefficients for the time series of site-observed WHD in eastern China and the $I_{Nino3.4}$, Iep, and Icp indices. Whether for EP or CP El Niño events, the indices feature a uniformly negative correlation with WHD at most of the stations in southern China. This result is in agreement with previous studies (e.g., Li et al., 2017; Zhao et al., 2018; He et al., 2019), which reported that the increase in precipitation over southern China due to the anomalous anticyclone over the West Pacific during the mature phase of El Niño events significantly reduced WHD in this region. However, the sign of the correlation coefficient between EP El Niño and WHD is completely opposite that between CP El Niño and WHD for the majority of sites in the JJJ region. For most sites, WHD is positively correlated with the Iep index (121 sites, accounting for 62.1% of all sites) but negatively correlated with the Icp index (126 sites, 64.6%). Considering the various inducements of haze pollution, such as local emissions, weather conditions, and topography, there may be some biases in correlation coefficients among different sites when examining the correlations between the single-site WHD and El Niño indices. However, the consistent positive and negative correlations at more than 60% of stations in response to EP and CP El Niño events support the opposite impacts of the two types of El Niño events on WHD in the JJJ region. The corresponding proportions increase to 70.5% and 86.2%, respectively, if we only count the stations where the correlations pass a significance level of 90%. As seen in Figure 1, the absolute values of the correlation coefficients at some stations exceed 0.4. There are statistically significant correlations between the site-averaged WHD in the JJJ region and the Iep and Icp indices ($p \leqslant 0.05$), with correlation coefficients of 0.16 and –0.2, respectively (Table 2). These low correlation values likely imply a mild impact of ENSO on WHD. However, the corresponding correlation coefficients reach 0.31 and –0.43, respectively, with a confidence level of 99%, when only considering the stations at which the correlations pass a significance

level of 90% (Fig. 1).

Figure 2 shows the composite anomalies of WHD at all sites over the JJJ region in different types of El Niño years relative to the 1961–2013 mean WHD. For the majority of stations in the JJJ region, WHD is increased in EP El Niño years (149 stations, 76.4% of all stations), with the maximum change exceeding 2.0 days (accounting for 17–79% of the average WHD; Fig. S2b). However, WHD is reduced at almost all stations over this region in CP El Niño years (172 stations, 91.8% of all stations), with the maximum change exceeding –2.0 days (accounting for –13% to –70% of the average WHD; Fig. S2c). For instance, in EP El Niño years, there are significant increases in WHD surrounding Beijing and Tianjin, in which the positive anomalies generally exceed 1.2 days. In CP El Niño years, the comparable negative WHD anomalies can be seen in the same region. The opposite differences in WHD corresponding to the two types of El Niño events are also apparent in the northwestern and northeastern parts of the JJJ region. The spatial correlation coefficient between the anomalous WHD in the JJJ region in both types of El Niño years reaches –0.71, which is significant at the 99% level.

The detailed statistics of WHD anomalies at all sites over the JJJ region in each El Niño year are shown by the box-and-whisker plots in Figure 3. As mentioned above, the WHD variations in the JJJ region are disturbed by local emissions, weather conditions, and topography. These result in a spread of distributions of WHD anomalies in response to individual EP or CP El Niño years. As seen in Figure 3a, the medians of WHD anomalies for all sites are below the zero line in all CP El Niño years, indicating a negative WHD anomaly for more than half of the sites. Although the medians of WHD anomalies fluctuate above and below the zero line in different EP El Niño years, the anomalies of WHD show obviously wider distributions in the positive range for all sites in each year, with the positive extremum exceeding 10 days in most EP El Niño years (data not shown in Fig. 3a). In addition, the distributions of WHD anomalies in different types of El Niño years also display interdecadal variations. The quasi-quadrennial mode was significantly strong, and EP events occurred more frequently during 1980–1999, corresponding to a larger proportion and higher extremum of positive WHD anomalies for all sites in the JJJ region. After 2000, the frequency of CP El Niño events was increased corresponding to the dominant quasi-biennial mode in the tropical Pacific, which led to a larger proportion and higher extremum of negative WHD anomalies in the JJJ region. This phenomenon may be attributable to the interdecadal transformation of the relative activity or stability between the two types of El Niño modes (Wang and Ren, 2017). Figure 3b also shows that the WHD anomalies are mainly located in the positive range in the EP El Niño years, but are obviously located in the negative range in the CP El Niño years.

In summary, the impacts of the two types of El Niño events on WHD are clearly opposite over the JJJ region. The EP El Niño events lead to increases in WHD in the JJJ region, whereas the CP El Niño events decrease WHD in this region. This is the reason why the correlation between the time series of WHD over North China and the El Niño indices was found to be statistically insignificant when considering the El Niño events as a whole in previous studies (e.g., Li et al., 2017; Zhao et al., 2018; He et al., 2019).

3.2 Anomalies of winter mean large-scale circulations for two types of El Niño

Next, we explore the physical mechanisms underlying the WHD changes in the JJJ region in response to EP and CP El Niño events from the perspective of large-scale circulation anomalies (Fig. 4). Previous studies have found that the severe haze events over North China in boreal winter were always accompanied by a decrease in northerly wind speed in the lower troposphere and weakening of the East Asian trough in the middle troposphere (Chen and Wang, 2015). The formation of heavy haze pollution over Beijing and its surroundings is significantly facilitated by the weakened EAWM, high-pressure anomalies at 500 hPa, and enhanced atmospheric stability (Zhang et al., 2014; Zhong et al., 2018).

The surface air temperature (SAT) generally increases over East Asia in the winters of EP El Niño years, especially in northern China, northeastern China, and eastern Siberia, with the maximum increase reaching 2 K (Fig. 4a). The SLP generally drops over East Asia. In particular, the SLP is decreased more significantly north of 30°N, with the maximum reaching –4 hPa in eastern Siberia (Fig. 4b). On the one hand, the worsening meteorological conditions, including near-

surface warming and low pressure, are not conducive to the southward movement of the Siberian high pressure system, thereby weakening the transport of the EAWM on aerosol pollutants over northern China. On the other hand, such conditions promote relatively stable circulation, which is conducive to the accumulation of aerosol pollutants. In addition, there is a significant positive anomaly of geopotential height at 500 hPa over the northwestern Pacific in the winters of EP El Niño years, with the maximum anomalies exceeding 20 gpm over southern Japan and the northwestern Pacific. These positive geopotential height anomalies also extend westward over northeastern and eastern China (Fig. 4c). At the same time, there is a negative geopotential height anomaly at 500 hPa over southwestern China. Consequently, such distribution of geopotential height anomalies results in an anomalous southerly wind in the middle and lower troposphere over northeastern and eastern China (Fig. 4d). The anomalous southerly wind weakens the seasonal prevailing northwesterly wind in the JJJ region, with the maximum decrease exceeding 0.5 m s^{-1}. This type of large-scale circulation anomaly suppresses the outward transport of aerosol pollutants in this region. Similar circulation anomalies were also found during the 2015/2016 super-strong EP El Niño event in an earlier study (Chang et al., 2016).

Compared to the EP El Niño years, there are larger increases in SAT and decreases in SLP over southern China in the winters of CP El Niño years, with the maximum changes reaching 0.8 K and –3 hPa, respectively, over the south of the Yangtze River (Fig. 4f and g). However, the positive SAT anomalies and negative SLP anomalies over northern China in the winters of CP El Niño years are apparently weaker than the corresponding changes in the winters of EP El Niño years (Fig. 4f and g). The SAT is significantly decreased in northeastern China and Siberia, with the largest negative anomalies reaching –2 K. Additionally, there is an anomalous negative geopotential height at 500 hPa over west of Lake Baikal and the Aleutian region, but a positive geopotential height at 500 hPa over southern Japan and the Korean peninsula in the winters of CP El Niño years (Fig. 4h). This leads to the westward shift of the East Asian trough (Jiang et al., 2017). As a result, there are northerly and northwesterly wind anomalies in the middle and lower troposphere north of 30°N in China, which significantly enhances the seasonal prevailing northerly wind (Fig. 4i). Such anomalous circulations are conducive to the outward transport of aerosol pollutants in the JJJ region. The monthly mean precipitation is significantly increased over eastern China in the winters of CP El Niño years, especially in the coastal regions of southeastern China, with the maximum changes exceeding 20 mm. Precipitation is generally increased over southern China, with the maximum changes exceeding 10 mm, but decreased slightly over central and northeastern China in the winters of EP El Niño years. The range of anomalous positive precipitation over the JJJ region is wider in CP El Niño years compared to that in EP El Niño years, although a comparable increase in precipitation over this region occurs with both types of El Niño years (Fig. 4e and j). Thus, the former is more conducive to enhancing the wet deposition of particulate matter.

Previous studies have emphasized the significant contributions to haze pollution of the formation of secondary inorganic and organic aerosols (Huang et al., 2014; Cheng et al., 2016; Wang et al., 2016a). Ma et al. (2017) attributed the elevation of $PM_{2.5}$ from heavy (150–250 μg m^{-3}) to severe (>250 μg m^{-3}) pollution to aerosol chemical conversion processes, which dominate the later stages of severe haze pollution. According to chamber studies and ambient measurements, the formation of secondary aerosols and their physical and chemical characterizations are markedly dependent on both temperature (Warren et al., 2009; Ding et al., 2011; Clark et al., 2016) and relative humidity (RH; Liu et al., 2011; Nguyen et al., 2011; Sun et al., 2013; Li et al., 2018). Given the lower temperature and ozone concentrations and higher coal consumption in winter in northern China (Chen et al., 2015), heterogeneous reactions related to sulfate and nitrate, rather than photochemical reactions, are considered mostly responsible for the increased $PM_{2.5}$ concentrations (Ma et al., 2017). This links the higher $PM_{2.5}$ concentrations with higher RH, as that factor contributes to these heterogeneous reactions (Cheng et al., 2016; Wang et al., 2016a). However, some studies have found nonsignificant or negative correlations between RH and WHD over northern China (Chen and Wang, 2015; Wu et al., 2016; He et al., 2019). Our results show apparently positive RH anomalies over eastern China in the winters of CP El Niño years. By contrast, increases in RH mainly occur over southern China, and RH is slightly increased or decreased over the JJJ region in the winters of EP El Niño years (Fig. S3). The changes in RH in the

mid-low troposphere over northern China in response to EP and CP El Niño years are not consistent with the corresponding variations in WHD in the JJJ region. This indicates that the regional transport of aerosol pollutants dominates the variations of WHD in the JJJ region in response to the two types of El Niño events, which supports the situation at the initial stage of haze occurrence as reported in Ma et al. (2017).

3.3 Anomalies in intraseasonal local synoptic conditions in the winters of different types of El Niño years

In this section, we further explore the different effects of the two types of El Niño events on WHD in the JJJ region from the perspective of changes in intraseasonal local synoptic conditions. Using the T-mode PCA and K-means cluster analysis methods, eight circulation types were identified over the JJJ region in winter. The effects of the two types of El Niño events on these circulation types were then compared. The changes in local synoptic conditions are defined as the differences between the results averaged in 10 EP (6 CP) El Niño years and the climatology.

Figures S4 and S5 show the climatological distributions of SLP, air temperature at 2 m, and wind at 10 m, respectively, over the JJJ region in winter for the eight circulation types. A larger northwest-southeast SLP gradient (Fig. S4a, b, c, and d) and a stronger northerly wind (Fig. S5a, b, c, and d) can be seen over the JJJ region for circulation Types 1, 2, 3, and 4. In particular, the high pressure system is stronger and broader (Fig. S4a and b), and the seasonal prevailing northerly and northwesterly winds are faster (Fig. S5a and b) over the northwestern part of the JJJ region for Types 1 and 2. This implies that the cold air is more active and the local aerosol pollutants are more easily transported outward under these circulation types. Conversely, there is an obviously smaller northwest-southeast SLP gradient (Fig. S4e, f, g, and h) and weaker seasonal prevailing northwesterly and westerly winds (Fig. S5e, f, g, and h) over the JJJ region for circulation Types 5, 6, 7, and 8. Above all, there is a significant belt of low pressure in the JJJ region, and the seasonal prevailing wind becomes a southwesterly wind in the southeastern part of this region under circulation Types 7 and 8. Such circulations with low pressure and weak wind not only suppress the southward movement of cold air but also promote atmospheric stability in the JJJ region. Consequently, the local aerosol pollutants are prone to accumulating. Therefore, Types 1–4 are defined as the clean circulation types and Types 5–8 are defined as the pollution ones in this study.

Table 3 shows the occurrence frequency of clean and pollution circulation types in winter corresponding to the climatological means and the two types of El Niño years. Compared to the climatological means, it is completely opposite for the composite changes in occurrence frequency of both pollution and clean circulation types between the two types of El Niño years. The total occurrence frequencies of clean and pollution circulation types are reduced by 0.2% and increased by 0.4%, respectively, in the winters of EP El Niño years. By contrast, the corresponding frequencies are increased by 0.6% and decreased by 0.5%, respectively, in the winters of CP El Niño years. These changes imply that the days conducive to the accumulation of local aerosol pollutants are increased in the winters of EP El Niño years, but the opposite occurs in the winters of CP El Niño years. Note that there are some differences among changes in the occurrence frequency of different pollution or clean circulation types. This leads to small magnitudes of the composite changes. However, the WHD anomalies corresponding to EP and CP El Niño years can generally be explained by the composite changes in occurrence frequency of both the pollution and clean circulation types.

In the winters of EP El Niño years, there are negative SLP anomalies over the northwestern and northern parts of the JJJ region but obviously positive SLP anomalies over the southeastern and eastern parts of this region under most circulation types, except for Types 1 and 6 (Fig. 5). Hence, the gradients of SLP are apparently decreased over the JJJ region for each circulation type in the winters of EP El Niño years relative to the climatological means (Fig. S4). Affected by this, southerly wind anomalies occur at the near-surface layer over the JJJ region for both clean and pollution circulation types (Fig. 7c). In addition, the anomalies of SAT over the JJJ region under most circulation types, except for Types 1 and 5, are mainly distributed in the positive anomaly range, indicating that the SAT is generally increased in this region (Fig. 7a). The above analyses show decreased SLP, reduced wind velocity, and increased SAT over the JJJ region under all circulation types in the

winters of EP El Niño years, which lead to a stable synoptic situation. This means that the suppression effects of pollution circulation types on the outward transport of local aerosol pollutants are enhanced over the JJJ region. At the same time, these anomalous synoptic conditions are not conducive to the southward activity of cold air, weakening the diffusion effect of clean circulation types on the local aerosol pollutants in this region.

In contrast, there are positive SLP anomalies over the northwestern and northern parts of the JJJ region, but negative SLP anomalies over the southeastern or southern parts of this region, under the clean circulation types in the winters of CP El Niño years, which increases the northwest-southeast SLP gradient (Fig. S4a–d and 6a–d). Correspondingly, the near-surface meridional wind anomalies over the JJJ region under the clean circulation types are mainly located in the negative anomaly range (Fig. 7d), which means that the seasonal prevailing wind is enhanced in this region. Moreover, the SAT anomalies are also distributed in the negative anomaly range under the clean circulation types (Fig. 7b), indicating a significant decrease in near-surface temperature over the JJJ region. These analyses show that the intensity of synoptic situations conducive to the outward transport of local aerosol pollutants is further enhanced over the JJJ region under the clean circulation types. This may be the reason for the reduction in WHD in this region.

In summary, there are significant differences between the impacts of the two types of El Niño events on the intraseasonal local synoptic conditions. These differences lead to opposite WHD anomalies over the JJJ region in response to different types of El Niño events. In the winters of EP El Niño years, the increase in WHD over the JJJ region may be related to the increased days of pollution circulation types, the decreased days of clean circulation types, the enhanced suppression effect of pollution circulation types on aerosol pollutants, and the weakened diffusion effect of clean circulation types. In the winters of CP El Niño years, the reductions in WHD in the JJJ region are mainly attributable to the increased days and intensity of clean circulation types and the decreased days of pollution circulation types.

4 Discussion and conclusions

Based on the long-term site observations of WHD from the CMA, the reanalysis datasets from the ECMWF, and the precipitation reanalysis data from the GPCC, this study explored the impacts of two types of El Niño events on WHD over China's JJJ region and the potential physical mechanisms underlying their differences. The conclusions and discussions are as follows.

The effects of the two types of El Niño events on WHD over the JJJ region are significantly different. There are statistically significant positive (negative) correlation coefficients between WHD over the JJJ region and the Iep (Icp) indices. However, the low correlations likely imply a mild impact of the ENSO on WHD. Correspondingly, WHD increases (decreases) over the JJJ region in the winters of EP (CP) El Niño years. Our results are obviously different from those in previous studies without distinguishing two types of El Niño events (e.g., Li et al., 2017; Sun et al., 2018; Zhao et al., 2018; He et al., 2019), which reported statistically insignificant effects of El Niño on winter haze pollution in North China.

Figure 8 shows the physical mechanisms corresponding to the effects of the EP and CP El Niño on WHD in the JJJ region. The changes in large-scale circulation at the near-surface and mid-low troposphere in East Asia are significantly different in response to the two types of El Niño events, which consequently leads to the opposite effects on WHD over the JJJ region. There are increases in SAT and decreases in SLP over North China in the winters of EP El Niño years. Simultaneously, the seasonal prevailing wind is weakened due to a large range of southerly wind anomalies over the mid-low troposphere in this region. These anomalies suggest that the activity of the EAWM is significantly suppressed and the intensity of cold air is weakened, both of which are conducive to the concurrent increases in WHD over the JJJ region. By contrast, meteorological anomalies, such as near-surface warming and low pressure, are apparent over southern China in the winters of CP El Niño years. The westward shift of the East Asian trough at 500 hPa leads to northerly and northwesterly wind anomalies over the mid-low troposphere in eastern China, which significantly enhances the seasonal prevailing wind. This may result in the

decrease in WHD over the JJJ region during the same period. Furthermore, the positive precipitation anomalies over eastern China are stronger in intensity and wider ranging in the winters of CP El Niño years, which also contributes to the reduction in WHD over the JJJ region.

Our results further indicate an increase in the total occurrence frequency of pollution circulation types and a decrease in that of clean circulation types in the winters of EP El Niño years. These changes support the accumulation and maintenance of local aerosol pollutants in the JJJ region. In addition, there are obvious synoptic condition anomalies, including the reduced SLP gradient, near-surface warming, and weakened northerly wind, over the JJJ region under all circulation types. These changes indicate the enhanced pollution and weakened clean circulation types in the winters of EP El Niño years, which may be one reason for the increased WHD over the JJJ region. Conversely, the reductions in WHD over the JJJ region are mainly attributable to the increase (decrease) in total occurrence frequency of clean (pollution) circulation types in the winters of CP El Niño years. These anomalous changes result in increased cold air days and thereby facilitate the outward transport of local aerosol pollutants. Meanwhile, the intensity of cold air is enhanced due to the larger SLP gradient, negative temperature anomalies, and stronger near-surface northerly winds over the JJJ region under the clean circulation types. These anomalies likely contribute to the reduction in WHD in this region.

In recent years, the air quality improvement projects implemented by China's government have effectively controlled the emissions of $PM_{2.5}$ in most areas of China (Zheng et el., 2018; Ding et al., 2019; Gui et al., 2019; Zhang et al., 2019b). However, haze pollution events continue to occur (Zhang et al., 2019a). The impacts of worsening meteorological conditions caused by annual climate change on the haze pollution process are worthy of concern. This study elucidates the potential physical mechanisms of WHD changes over the JJJ region in response to two types of El Niño events from the perspectives of large-scale circulation and local synoptic condition anomalies. As reported by Yu et al. (2019), we further emphasized the importance of distinguishing the effects of the two types of El Niño events on winter haze pollution in North China. This study has certain implications for further understanding the impact of climate changes on air pollution in China's typical regions. Note that El Niño has the potential to change the composition and size distribution of aerosols by affecting aerosol transport, deposition, and chemical reactions, which are central to haze pollution (Li et al., 2011; Shaheen et al., 2013; Rajeev et al., 2016; Jayarathne et al., 2018). According to our results, we prefer to attribute the variations in WHD in the JJJ region in El Niño years to the impact of El Niño on the regional transport of aerosols. However, overall aerosol processes related to El Niño could not be precisely characterized at present, as there are few long-term, large-scale observations of aerosol composition, particle types, and size distribution in China. More detailed analyses need to be completed by gathering more observations and performing more sensitive simulations in future work. In addition, winter haze pollution in China may also be affected by multiple-timescale climate change factors, including the EAWM (Kim et al., 2016), Arctic Oscillation (Chen et al., 2013), Arctic sea ice (Wang and Chen, 2016b), Tibetan Plateau heat source (Xu et al., 2016), and interdecadal variation in snow cover (Yin et al., 2018). Future research should consider how to quantify the comprehensive contributions of different climate change factors to haze pollution in China.

Data availability

The monthly haze days dataset can be acquired from http://data.cma.cn/data/cdcindex/cid/6d1b5efbdcbf9a58.html. The monthly Niño3, Niño4, and Niño3.4 indices are available at http://cmdp.ncc-cma.net/download/Monitoring/Index/M_Oce_Er.txt. Daily and monthly ERA-40 and ERA-Interim reanalysis data are available at https://www.ecmwf.int/en/forecasts/datasets/browse-reanalysis-datasets. The global land surface precipitation data can be acquired from https://climatedataguide.ucar.edu/climate-data.

Author contributions

ZW conceived the study. XY, ZW, and HZ performed the analysis and led the manuscript writing. All authors provided

comments and contributed to the text.

Competing interests

The authors declare that they have no conflict of interest.

Acknowledgments

This study was supported by the key National Natural Science Foundation of China (91644211) and National Key Research and Development Program of China (2016 YFC0203306).

References

Ashok, K., Behera, S. K., and Rao, S. A.: El Niño Modoki and its possible teleconnection. Journal of Geophysical Research: Oceans, 112, C11007, doi:10.1029/2006jc003798, 2007.

Bejarano, L. and Jin, F. F.: Coexistence of equatorial coupled modes of ENSO. Journal of Climate, 21(12): 3051-3067, doi:10.1175/2007jcli1679.1, 2008.

Cai, W. J., Li, K., Liao, H., Wang, H. J., and Wu, L. X.: Weather conditions conducive to Beijing severe haze more frequent under climate change. Nature Climate Chang, 7(4), 257–262, doi:10.1038/nclimate3249, 2017.

Cai, W. J., Wang, G. J., Dewitte, B., Wu, L. X., Santoso, A., Takahashi, K, Yun, Y., Carréric, A., and McPhaden, J. M.: Increased variability of eastern Pacific El Niño under greenhouse. Nature, 564(7735), 201-206, doi:10.1038/s41586-018-0776-9, 2018.

Cane, M. A.: The evolution of El Niño, past and future. Earth and Planetary Science Letters, 230(3), 227–240, doi:10.1016/j.epsl.2004.12.003, 2005.

Chang, L. Y., Xu, J. M., Tie, X. X., and Wu, J. B.: Impact of the 2015 El Nino event on winter air quality in China. Scientific Reports, 6(1):34275, doi:10.1038/srep34275, 2016.

Chen, H. P. and Wang, H. J.: Haze Days in North China and the associated atmospheric circulations based on daily visibility data from 1960 to 2012. Journal of Geophysical Research Atmospheres, 120(12):5895-5909, doi:10.1002/2015jd023225, 2015.

Chen, X., Huang, F. X., Xia, X. Q., Cao, J. and Xu, X. B.: Analysis of tropospheric ozone long-term changing trends and affecting factors over northern China (in Chinese). Chinese Science Bulletin, 60(27): 2659-2666, doi: 10.1360/N972015-00155, 2015.

Chen, W., Lan, X. Q., Wang, L., and Ma, Y.: The combined effects of the ENSO and the Arctic Oscillation on the winter climate anomalies in East Asia. Chinese Science Bulletin, 58(12):1355-1362, doi:10.1007/s11434-012-5654-4, 2013.

Cheng, Y. F., Zheng, G. J., Wei, C., Mu, Q., Zheng, B., Wang, Z. B., Gao, M., Zhang, Q., He, K. B., Carmichael, G., PÖschl, U. and Su, H.: Reactive nitrogen chemistry in aerosol water as a source of sulfate during haze events in China. Science Advances, 2(12), e1601530-e1601530, doi: 10.1126/sciadv.1601530, 2016.

Clark, C. H., Kacarab, M., Nakao, S., Asa-Awuku, A., Sato, K. and Cocker, D. R.: Temperature Effects on Secondary Organic Aerosol (SOA) from the Dark Ozonolysis and Photo-Oxidation of Isoprene. Environmental Science & Technology, 50(11): 5564-5571, doi: 10.1021/acs.est.5b05524, 2016.

Ding, A. J., Huang, X., Nie, W., Chi, X. G., Xu, Z., Zheng, L. F., Xu, Z. N., Xie, Y. N., Qi, X. M., Shen, Y. C., Sun, P., Wang, J. P., Wang, L., Sun, J. N., Yang, X. Q., Qin, W., Zhang, X. Z., Cheng, W., Liu, W. J., Pan, L. B., and Fu, C. B.: Significant reduction of $PM_{2.5}$ in eastern China due to regional-scale emission control: evidence from SORPES in 2011–2018. Atmospheric Chemistry and Physics, 19(18): 11791–11801, doi:10.5194/acp-19-11791-2019, 2019.

Ding, X., Wang, X. M. and Zheng, M.: The influence of temperature and aerosol acidity on biogenic secondary organic

aerosol tracers: Observations at a rural site in the central Pearl River Delta region, South China. Atmospheric Environment, 45(6): 1303-1311, doi: 10.1016/j.atmosenv.2010.11.057, 2011.

Doyle, M. and Dorling, S.: Visibility trends in the UK 1950-1997. Atmospheric Environment, 36(19): 3161-3172, doi: 10.1016/s1352-2310(02)00248-0, 2002.

Feng, J., Li, J. P., Zhu, J. L., and Liao, H.: Influences of El Niño Modoki event 1994/1995 on aerosol concentrations over southern China. Journal of Geophysical Research Atmospheres, 121 (4), 1637–1651, doi:10.1002/2015jd023659, 2016a.

Feng, J., Zhu, J. L., and Li, Y.: Influences of El Niño on aerosol concentrations over eastern China. Atmospheric Science Letters, 17 (7), 422-430, doi:10.1002/asl.674, 2016b.

Gao, H. and Li, X.: Influences of El Nino Southern Oscillation events on haze frequency in eastern China during boreal winters. International Journal of Climatology, 35 (9), 2682–2688, doi:10.1002/joc.4133, 2015.

Gao, J. H., Woodward, A., Vardoulakis, S., Vardoulakis, S., Kovats, S., Wilkinson, P., Li, J. P., Xu, L., Li, J., Yang, J., Li, J., Cao, L. N., Liu, X. B., Wu, H. X., and Liu, Q. Y.: Haze, public health and mitigation measures in China: A review of the current evidence for further policy response. Science of The Total Environment, 578: 148-157, doi: 10.1016/j.scitotenv.2016.10.231, 2017.

Gui, K., Che, H. Z., Wang, Y. Q., Wang, H., Zhang, L., Zhao, H. J., Zheng, Y., Sun, T. Z., and Zhang, X. Y.: Satellite-derived $PM_{2.5}$ concentration trends over Eastern China from 1998 to 2016: Relationships to emissions and meteorological parameters. Environmental Pollution, 247: 1125–1133, doi:10.1016/j.envpol.2019.01.056, 2019.

He, C., Liu, R., Wang, X. M., Liu, S. C., Zhou, T. J., and Liao, W. H.: How does El Niño-Southern Oscillation modulate the interannual variability of winter haze days over eastern China? Science of The Total Environment, 651,1892-1902, doi:10.1016/j.scitotenv.2018.10.100, 2019.

He, J. J., Gong, S. L., Liu, H. L., An, X. Q., Zhao, S. P., Wu, L., Song, C. B., Zhou, C. H., Wang, J., Yin, C. M., and Yu, L. J.: Influences of meteorological conditions on interannual variations of particulate matter pollution during winter in the Beijing–Tianjin–Hebei area. Journal of Meteorological Research, 31(6):1062-1069, doi:10.1007/s13351-017-7039-9, 2017a.

He, J. J., Gong, S. L., Yu, Y., Yu, L. J., Wu, L., Mao, H. J., Song, C. B., Zhao, S. P., Liu, H. L., Li, X. Y., and Li, R. P.: Air pollution characteristics and their relation to meteorological conditions during 2014-2015 in major Chinese cities. Environmental Pollution, 223:484-496, doi:10.1016/j.envpol.2017.01.050, 2017b.

He, J. J., Gong, S. L., Zhou, C. H., Lu, S. H., Chen, Y., Yu, Y., Zhao, S. P., Yu, L. J., and Yin, C. M.: Analyses of winter circulation types and their impacts on haze pollution in Beijing. Atmospheric Environment, 192, 94-103, doi:10.1016/j.atmosenv.2018.08.060, 2018.

Huang, R. J., Zhang, Y. L., Bozzetti, C., Ho, K. F., Cao, J. J., Han, Y. M., Daellenbach, K. R., Slowik, J. G., Platt, S. M., Canonaco, F., Zotter, P., Wolf, R., Pieber, S. M., Bruns, E. A., Crippa, M., Ciarelli, G., Piazzalunga, A., Schwikowski, M., Abbaszade, G., Schnelle-Kreis, J., Zimmermann, R., An, Z. S., Szidat, S., Baltensperger, U., Haddad, I. E. and Prévôt, A. S. H.: High secondary aerosol contribution to particulate pollution during haze events in China. Nature, 514(7521), 218-222, doi:10.1038/nature13774, 2014.

Huth, R.: An intercomparison of computer-assisted circulation classification methods. International Journal of Climatology, 16(8), 893-922, doi:10.1002/(sici)1097-0088(199608)16:8<893::aid-joc51>3.0.co;2-q, 1996.

Jayarathne, T., Stockwell, C. E., Gilbert, A. A., Daugherty, K., Cochrane, M. A., Ryan, K. C., Putra, E. I., Saharjo, B. H., Nurhayati, A. D., Albar, I., Yokelson, R. J. and Stone, E. A.: Chemical characterization of fine particulate matter emitted by peat fires in Central Kalimantan, Indonesia, during the 2015 El Niño. Atmospheric Chemistry and Physics, 18(4), 2585-2600, doi:10.5194/acp-18-2585-2018, 2018.

Jiang, Y. Q., Yang, X. Q., Liu, X. H., Yang, D. J., Sun, X. G., Wang, M. H., Ding, A. J., Wang, T. J., and Fu, C. B.: Anthropogenic aerosol effects on East Asian winter monsoon: The role of black carbon induced Tibetan Plateau warming. Journal of Geophysical Research: Atmospheres, 122(11), 5883-5902, doi:10.1002/2016jd026237, 2017.

Kim, J. W., An, S. I., Jun S. Y., Park, H. J., and Yeh, S. W.: ENSO and East Asian winter monsoon relationship modulation associated with the anomalous northwest Pacific anticyclone. Climate Dynamics,49(4):1157-1179, doi:10.1007/s00382-016-3371-5, 2017.

Larkin, N. K. and Harrison, D. E.: On the definition of El Niño and associated seasonal average U.S. weather anomalies. Geophysical Research Letters, 32(13), 435–442, doi:10.1029/2005gl022738, 2005.

Levine, A. F. and Jin, F. F.: Noise-induced instability in the ENSO recharge oscillator. Journal of the Atmospheric Sciences, 67(2): 529-542, doi:10.1175/2009jas3213.1, 2010.

Li, J., Carlson, B. E. and Lacis, A. A.: El Niño-Southern Oscillation correlated aerosol ÅngstrÖm exponent anomaly over the tropical Pacific discovered in satellite measurements. Journal of Geophysical Research, 116(D20), doi:10. 1029/2011jd015733, 2011.

Li, K., Liao, H., Cai, W. J., and Yang, Y.: Attribution of Anthropogenic Influence on Atmospheric Patterns Conducive to Recent Most Severe Haze Over Eastern China. Geophysical Research Letters, 45(4): 2072-2081, doi:10.1002/2017gl076570, 2018.

Li, Q., Zhang, R. H., and Wang, Y.: Interannual variation of the wintertime fog–haze days across central and eastern China and its relation with East Asian winter monsoon. International Journal of Climatology, 36(1), 346–354, doi:10.1002/joc.4350, 2016.

Li, S. L., Han, Z., and Chen, H. P.: A comparison of the effects of interannual Arctic sea ice loss and ENSO on winter haze days: observational analyses and AGCM simulations. Journal of Meteorological Research, 31(5), 820–833, doi:10.1007/s13351-017-7017-2, 2017.

Li, Z. Y., Smith, K. A. and Cappa, C. D.: Influence of relative humidity on the heterogeneous oxidation of secondary organic aerosol. Atmospheric Chemistry and Physics, 18(19), 14585-14608, doi: 10.5194/acp-18-14585-2018, 2018.

Liu, D. and Gao, S. C.: Determining the number of clusters in K-means clustering algorithm. Silicon Valley, 6: 38-39, 2011.

Liu, P. F., Zhao, C. S., GÖbel, T., Hallbauer, E., Nowak, A., Ran, L., Xu, Y. W., Deng, Z. Z., Ma, N., Mildenberger, K., Henning, S., Stratmann, F. and Wiedensohler, A.: Hygroscopic properties of aerosol particles at high relative humidity and their diurnal variations in the North China Plain. Atmospheric Chemistry and Physics, 11(7): 3479-3494, doi: 10.5194/acp-11-3479-2011, 2011.

Liu, T. T., Gong, S. L., He, J. J., Yu, M., Wang, Q. F., Li, H. R., Liu, W., Zhang, J., Li, L., Wang, X. G., Li, S. L., Lu, Y. L., Du, H. T., Wang, Y. Q., Zhou, C. H., Liu, H. L., and Zhao, Q. C.: Attributions of meteorological and emission factors to the 2015 winter severe haze pollution episodes in China's Jing-Jin-Ji area. Atmospheric Chemistry and Physics, 17(4), 2971-2980, doi:10.5194/acp-17-2971-2017, 2017.

Ma, Q. X., Wu, Y. F., Zhang, D. Z., Wang, X. J., Xia, Y. J., Liu, X. Y., Tian, P., Han, Z. W., Xia, X. G., Wang, Y., and Zhang, R. J.: Roles of regional transport and heterogeneous reactions in the $PM_{2.5}$ increase during winter haze episodes in Beijing. Science of the Total Environment, 599-600, 246-253, doi: 10.1016/j.scitotenv.2017.04.193, 2017.

Miao, Y. C., Guo, J. P., Liu, S. H., Li, Z. Q., Zhang, W. C., and Zhai, P. M.: Classification of summertime synoptic patterns in Beijing and their associations with boundary layer structure affecting aerosol pollution. Atmospheric Chemistry and Physics, 17(4), 3097–3110, doi:10.5194/acp-17-3097-2017, 2017.

Mu, M. and Ren, H. L.: Enlightenments from researches and predictions of 2014-2016 super El Niño event. Science China Earth Sciences, 60(9): 1569-1571, doi:10.1007/s11430-017-9094-5, 2017.

Nguyen, T. B., Roach, P. J., Laskin, J., Laskin, A. and Nizkorodov, S. A.: Effect of humidity on the composition of isoprene photooxidation secondary organic aerosol. Atmospheric Chemistry and Physics, 11(14): 6931-6944, doi:10.5194/acp-11-6931-2011, 2011.

Rajeev, P., Rajput, P. and Gupta, T.: Chemical characteristics of aerosol and rain water during an El Niño and PDO influenced Indian summer monsoon. Atmospheric Environment, 145, 192-200, doi:10.1016/j.atmosenv.2016.09.026, 2016.

Ren, H. L., Sun, C. H., Ren, F. M., Yuan, Y., Lu, B., Tian, B., Zuo, J. Q., Liu, Y., Cao, L, Han, R. Q., Jia, X. L. and Liu, C. Z.: Identification method for El Niño/La Niña events. The People's Republic China's National Standard GB/T 33666-2017, May 2017. Beijing: Standards Press of China, 1-6, 2017.

Richman, M. B.: Obliquely rotated principal components: an improved meteorological map typing technique? Journal of Applied Meteorology, 20(10), 1145-1159, doi:10.1175/1520-0450(1981)020<1145:orpcai>2.0.co;2, 1981.

Roberts, A., Guckenheimer, J., Widiasih, E., Timmermann, A., and Joner, C. K. R. T.: Mixed-mode oscillations of El Niño–southern oscillation. Journal of the Atmospheric Sciences, 73(4): 1755-1766, doi:10.1775/jas-d-15-0191.1, 2016.

Schichtel, B. A., Husar, R. B., Falke, S. R. and Wilson, W. E.: Haze trends over the United States, 1980-1995. Atmospheric Environment, 35(30), 5205-5210, doi:10.1016/s1352-2310(01)00317-x, 2001.

Schneider, U., Becker, A., Finger, P., Christoffer, A. M., Ziese, M., and Rudolf, B.: GPCC's new land surface precipitation climatology based on quality-controlled in situ data and its role in quantifying the global water cycle. Theoretical and Applied Climatology, 115(1-2): 15-40, doi:10.1007/s00704-013-0860-x, 2014.

Shaheen, R., Abauanza, M., Jackson, T. L., McCabe, J., Savarino, J. and Thiemens, M. H.: Tales of volcanoes and El- Niño southern oscillations with the oxygen isotope anomaly of sulfate aerosol. Proceedings of the National Academy of Sciences, 110(44):17662-17667, doi:10.1073/pnas. 1213149110, 2013.

Sun, J. R., Li, H. Y., Zhang, W. J., Li, T. R., Zhao, W., Zuo, Z. Y., Guo, S., Wu, D., and Fan, S. J.: Modulation of the ENSO on Winter Aerosol Pollution in the Eastern Region of China. Journal of Geophysical Research: Atmospheres, 11: 952-969, doi:10.1029/2018jd028534, 2018.

Sun, Y. L., Wang, Z. F., Fu, P. Q., Jiang, Q., Yang, T., Li, J. and Ge, X. L.: The impact of relative humidity on aerosol composition and evolution processes during wintertime in Beijing, China. Atmospheric Environment, 77, 927-934, doi: 10.1016/j.atmosenv.2013.06.019, 2013.

Timmermann, A., An, S. I., Kug, J. S., Jin, F. F., Cai, W. J., Capotondi, A., Cobb, K., Lengaigne, M., McPhaden, M. J., Stuecker, M. F., Stein, K., Wittenberg, A. T., Yun, K. S., Bayr, T., Chen, H. C., Chikamoto, Y., Dewitte, B., Dommenget, D., Grothe, P., Guilyardi, E., Ham, Y. G., Hayashi, M., Ineson, S., Kang, D., Kim, S., Kim, W. M., Lee, J. L., Li, T., Luo, J. J., McGregor, S., Planton, Y., Power, S., Rashid, H., Ren, H. L., Santoso, A., Takahashi, K., Todd, A., Wang, G. M., Wang, G. J., Xie, R. H., Yang, W. H., Yeh, S. W., Yoon, J., Zeller, E., and Zhang, X. B.: El Niño–Southern Oscillation complexity. Nature, 559(7715): 535-545, doi:10.1038/s41586-018-0252-6, 2018.

Wang, G. H., Zhang, R. Y., Gomez, M. E., Yang, L. X., Zamora, M. L., Hu, M., Lin, Y., Peng, J. F., Guo, S., Meng, J. J., Li, J. J., Cheng, C. L., Hu, T. F., Ren, Y. Q., Wang, Y. S., Gao, J., Cao, J. J., An, Z. S., Zhou, W. J., Li, G. H., Wang, J. Y., Tian, P. F., Marrero-Ortiz, W., Secrest, J., Du, Z. F., Zheng, J., Shang, D. J., Zeng, L. M., Shao, M., Wang, W. G., Huang, Y., Wang, Y., Zhu, Y. J., Li, Y. X., Hu, J. X., Pan, B. W., Cai, L., Cheng, Y. T., Ji, Y. M., Zhang, F., Rosenfeld, D., Liss, P. S., Duce, R. A., Kolb, C. E. and Molina, M. J.: Persistent sulfate formation from London Fog to Chinese haze. Proceedings of the National Academy of Sciences, 113(48), 13630-13635, doi: 10.1073/pnas.1616540113, 2016a.

Wang, H. J. and Chen, H. P.: Understanding the recent trend of haze pollution in eastern China: roles of climate change. Atmospheric Chemistry and Physics, 16: 4205–4211, doi:10.5194/acp-2015-1009, 2016b.

Wang, R. and Ren, H. L.: The linkage between two ENSO types/modes and the interdecadal changes of ENSO around the year 2000. Atmospheric and Oceanic Science Letters, 10(2): 168-174, doi:10.1080/16742834.2016.1258952, 2017.

Warren, B., Austin, R. L., and Cocker, D. R.: Temperature dependence of secondary organic aerosol. Atmospheric Environment, 43(22-23): 3548-3555, doi: 10.1016/j.atmosenv. 2009.04.011, 2009.

Wu, D., Wu, X. J., Li, F., Tan, H. B., Chen, J., Cao, Z. Q., Sun, X., Chen, H. H. and Li, H. Y.: Temporal and spatial variation of haze during 1951-2005 in Chinese mainland. Acta Meteorological Sinica, 68(5):680-688, doi:10.3788/gzxb20103906.0998, 2010.

Wu, P., Ding, Y. H., Liu, Y. J. and Li, X. C.: Influence of the East Asian winter monsoon and atmospheric humidity on the

wintertime haze frequency over central-eastern China. Acta. Meteorologica. Sinica., 74(3): 352-366, doi: 10.11676/qxxb2016.029, 2016.

Wyrtki, K.: El Niño-the dynamic response of the equatorial Pacific Ocean to atmospheric forcing. Journal of Physical Oceanography 5, 572-584, 1975.

Xu, X. D., Zhao, T. L., Liu, F., Gong, S. L., Kristovich, D., Lu, C., Guo, Y., Cheng, X., Wang, Y., and Ding, G.: Climate modulation of the Tibetan Plateau on haze in China. Atmospheric Chemistry and Physics, 16(3): 1365–1375, doi:10.5194/acp-16-1365-2016, 2016.

Yin, Z. C. and Wang, H. J.: The Strengthening Relationship between Eurasian Snow Cover and December Haze Days in Central North China after the Mid-1990s. Atmospheric Chemistry and Physics, 18,4753-4763, doi:10.5194/acp-2017-1055, 2018.

Yuan, Y. and Song, G.: Impacts of Different Types of El Niño on the East Asian Climate: Focus on ENSO Cycles. Journal of Climate, 25(21): 7702-7722, doi: 10.1175/jcli-d-11-00576.1, 2012.

Yu, X. C., Wang, Z. L., Zhang, H., and Zhao, S. Y.: Impacts of different types and intensities of El Niño events on winter aerosols over China. Science of The Total Environment, 655, 766-780, doi:10.1016/j.scitotenv.2018.11.090, 2019.

Zhang, J. P., Zhu, T., Zhang, Q. H., Li, C. C., Shu, H. L., Ying, Y., Dai, Z. P., Wang, X., Liu, X. Y., Liang, A. M., Shen, H. X., and Yi, B. Q.: The impact of circulation patterns on regional transport pathways and air quality over Beijing and its surroundings. Atmospheric Chemistry and Physics, 12, 5031–5053, doi:10.5194/acp-12-5013-2012, 2012.

Zhang, Q., Zheng, Y. X., Tong, D., Shao, M., Wang, S. X., Zhang, Y. H., Xu, X. D., Wang, J. N., He, H., Liu, W. Q., Ding, Y. H., Lei, Y., Li, J. H., Wang, Z. F., Zhang, X. Y., Wang, Y. S., Cheng, J., Liu, Y., Shi, Q. R., Yan, L., Geng, G. N., Hong, C. P., Li, M., Liu, F., Zheng, B., Cao, J. J., Ding, A. J., Gao, J., Fu, Q. Y., Huo, J. T., Liu, B. X., Liu, Z. R., Yang, F. M., He, K. B., and Hao, J. M.: Drivers of improved $PM_{2.5}$ air quality in China from 2013 to 2017. Proceedings of National Academy of Sciences, 116(49), 24463–2446, doi:10.1073/pans.1907956116, 2019.

Zhang, R. H., Li, Q., and Zhang, R. N.: Meteorological conditions for the persistent severe fog and haze event over eastern China in January 2013. Science China Earth Sciences, 57(1):26-35, doi:10.1007/s11430-013-4774-3, 2014.

Zhang, X. Y., Zhong, J. T., Wang, J. Z., Wang, Y. Q., and Liu, Y. J.: The interdecadal worsening of weather conditions affecting aerosol pollution in the Beijing area in relation to climate warming. Atmospheric Chemistry and Physics, 18(8), 5991-5999, doi:10.5194/acp-18-5991-2018, 2018.

Zhang, X. Y., Xu, X. D., Ding, Y. H., Liu, Y. J., Zhang, H. D., Wang, Y. Q., and Zhong, J. T.: The impact of meteorological changes from 2013 to 2017 on $PM_{2.5}$ mass reduction in key regions in China. Science China Earth Sciences, 49: 1-18, doi:10.1007/s11430-019-9343-3, 2019.

Zhao, S. Y., Zhang, H., and Xie, B.: The effects of El Niño-South Oscillation on the winter haze pollution of China. Atmospheric Chemistry and Physics, 18, 1863–1877, doi:10.5194/acp-18-1863-2018, 2018.

Zheng, B., Tong, D., Li, M., Liu, F., Hong, C. P., Geng, G. N., Li, H. Y., Li, X., Peng, L. Q., Qi, J., Yan, L., Zhang, Y. X., Zhao, H. Y., Zheng, Y. X., He, K. B., and Zhang, Q.: Trends in China's anthropogenic emissions since 2010 as the consequence of clean air actions. Atmospheric Chemistry and Physics, 18(19): 14095–14111, doi:10.5194/acp-18-14095-2018, 2018.

Zhong, J. T., Zhang, X. Y., Dong, Y. S., Wang, Y. Q., Liu, C., Wang, J. Z., Zhang, Y. M., and Che, H. C.: Feedback effects of boundary-layer meteorological factors on cumulative explosive growth of $PM_{2.5}$ during winter heavy pollution episodes in Beijing from 2013 to 2016. Atmospheric Chemistry and Physics, 18(1), 247-258, doi:10.5194/acp-18-247-2018, 2018.

Table 1: The classification of El Niño events

Eastern Pacific (EP)	Central Pacific (CP)
1963/1964、1965/1966、1972/1973、1976/1977、1979/1980、1982/1983、1986/1988、1991/1992、1997/1998、2006/2007	1968/1970、1977/1978、1994/1995、2002/2003、2004/2005、2009/2010

585

590

595

600

605

610

Table 2: Correlation coefficients between the time series of site-averaged winter haze days in China's JJJ region and different types of El Niño indices. The values in parentheses indicate the correlation coefficients and confidence levels when only considering the stations where the correlations pass a 90% significance level.

	Nino3.4	Iep	Icp
Cor	0.04（0.06）	0.16（0.31）	-0.20（-0.43）
P	0.65（0.45）	0.05（<0.01）	0.01（<0.01）

Table 3: The occurrence frequencies of each circulation type in winter for climatology and two types of El Niño years (unit: %). The values in parentheses represent changes relative to the climatological means.

		climatology	EP El Niño year	CP El Niño year
Clean circulation types	T1	10.3%	10.6% (+0.3%)	10.3% (+0%)
	T2	13.1%	13.6% (+0.5%)	14.0% (+0.9%)
	T3	14.8%	14.7% (-0.1%)	14.9% (+0.1%)
	T4	15.6%	14.7% (-0.9%)	15.2% (-0.4%)
	Total	53.8%	53.6% (-0.2%)	54.4 % (+0.6%)
Pollution circulation types	T5	17.2%	16.6% (-0.6%)	14.9% (-2.3%)
	T6	13.5%	13.0% (-0.5%)	15.1% (+1.6%)
	T7	10.6%	10.2% (-0.4%)	11.3% (+0.7%)
	T8	4.8%	6.7% (+1.9%)	4.3% (-0.5%)
	Total	46.1%	46.5% (+0.4%)	45.6 % (-0.5%)

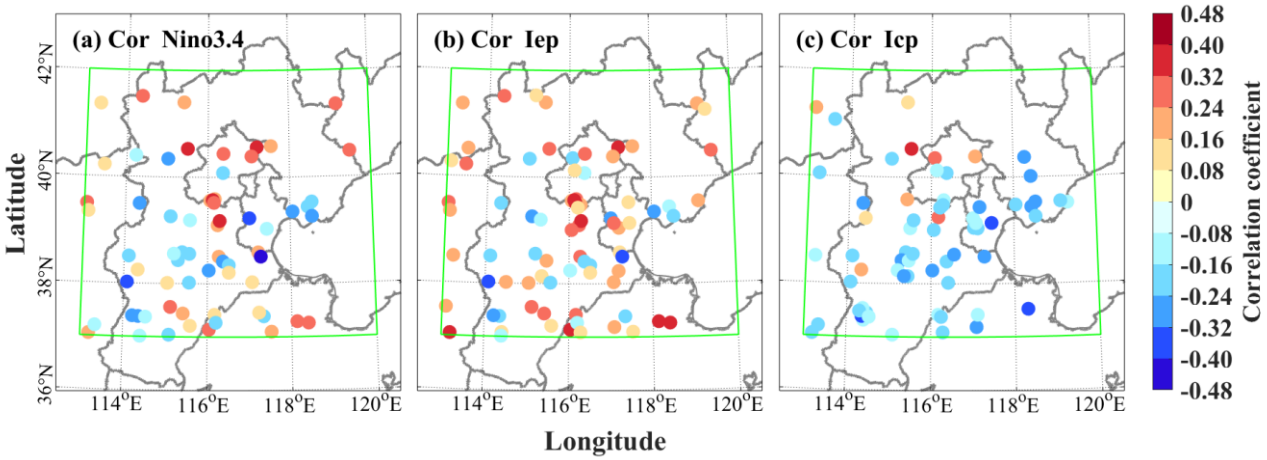

Figure 1: Correlation coefficients between the time series of site-observed winter haze days in JJJ region and (a) $I_{Nino3.4}$, (b) Iep, and (c) Icp indices. The correlations at these sites are significant at 90% confidence level. The green box represents the domain of the JJJ region (37–42°N, 113–120°E) in this study.

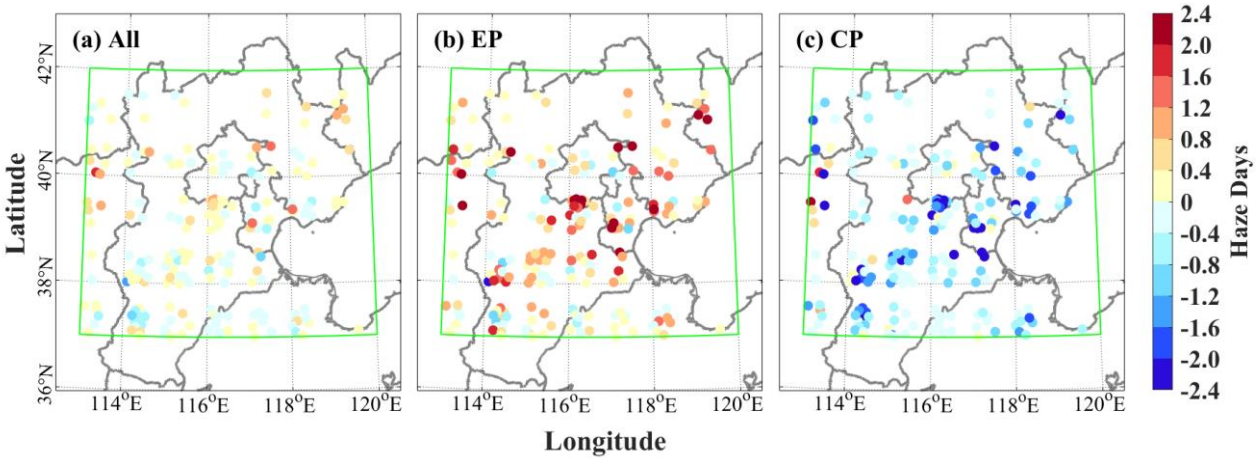

Figure 2: Composite changes of winter haze days at all sites over JJJ region in (a) all El Niño, (b) EP El Niño, and (c) CP El Niño years relative to the 1961-2013 mean winter haze days (unit: day). The green box represents the domain of the JJJ region (37–42°N, 113–120°E) in this study.

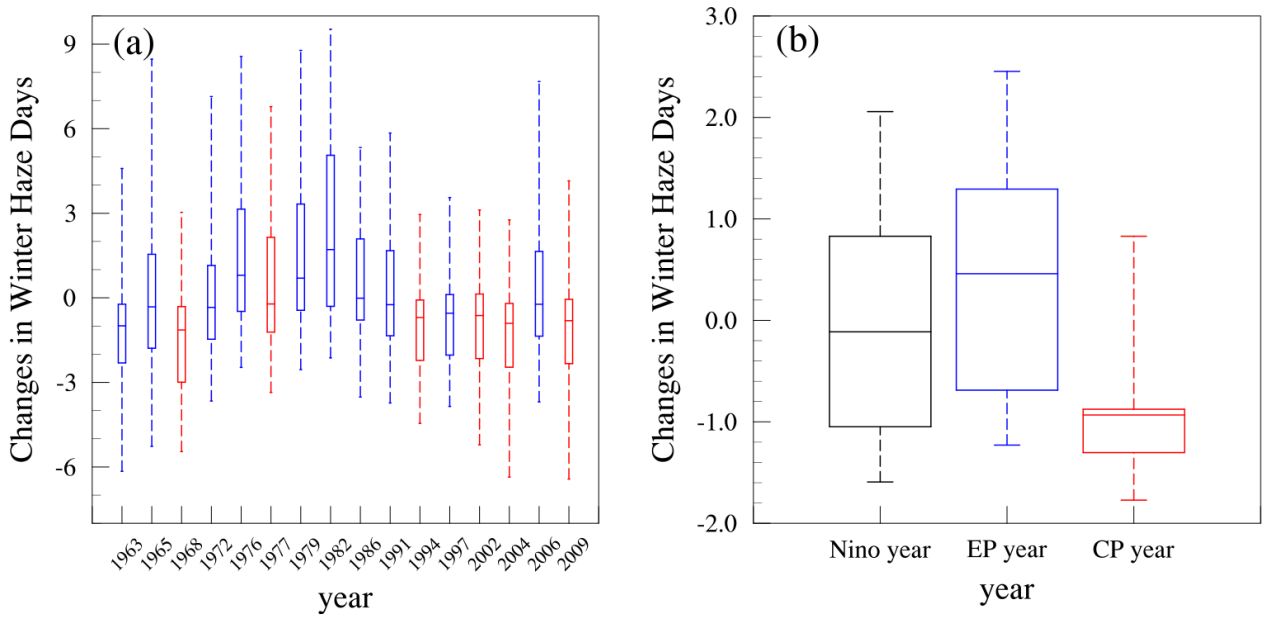

Figure 3: Box-and-whisker plots of (a) WHD anomalies at all sites over JJJ region in each El Niño year and (b) site-averaged WHD anomalies in different types of El Niño years (unit: day). Each site-averaged WHD anomaly was sampled from a single El Niño year and all these anomalies were divided into groups named as Nino year, EP year, and CP year. The blue, red, and black lines represent the EP, CP, and all El Niño years, respectively. Each box-and-whisker consists of the 5th percentile (the lower point of whisker), 25th quantile (the lower border of box), median (horizontal line in the middle of box), 75th quantile (the upper border of box) and 95th percentile (the upper point of whisker).

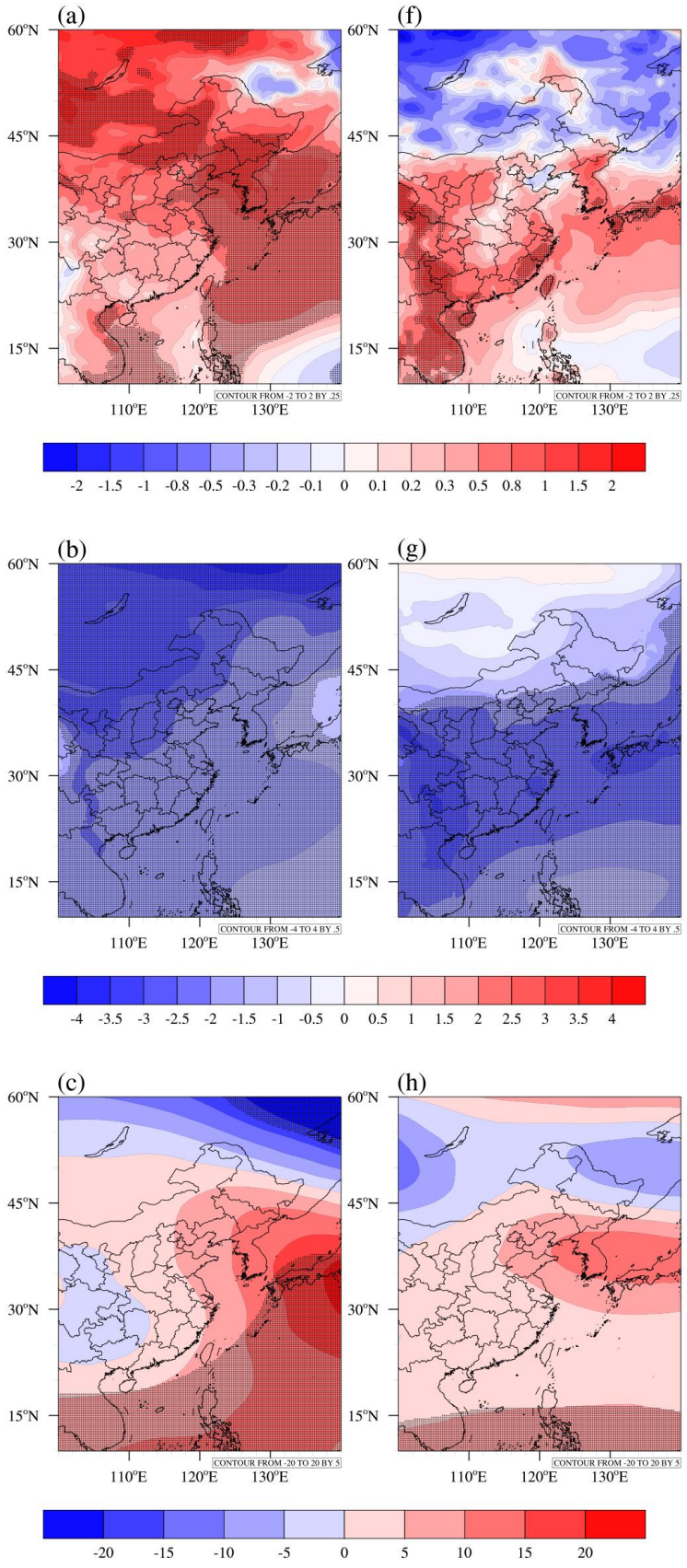

Figure 4: Winter mean changes in (a, f) air temperature at 2 m (unit: K), (b, g) sea level pressure (unit: hPa), (c, h) geopotential height at 500 hPa (unit: gpm), (d, i) wind averaged from 1000 hPa to 850 hPa (The arrows represent wind vectors and the contours represent wind velocities, unit: m s^{-1}), and (e, j) precipitation (unit: mm) in responses to the two types of El Niño. The left (a-e) and right (f-j) panels represent the differences averaged in 10 EP El Niño and 6 CP El Niño years, respectively, relative to the 1961-2013 climatological means. The dots indicate significance at ≥ 90% confidence level from the t test.

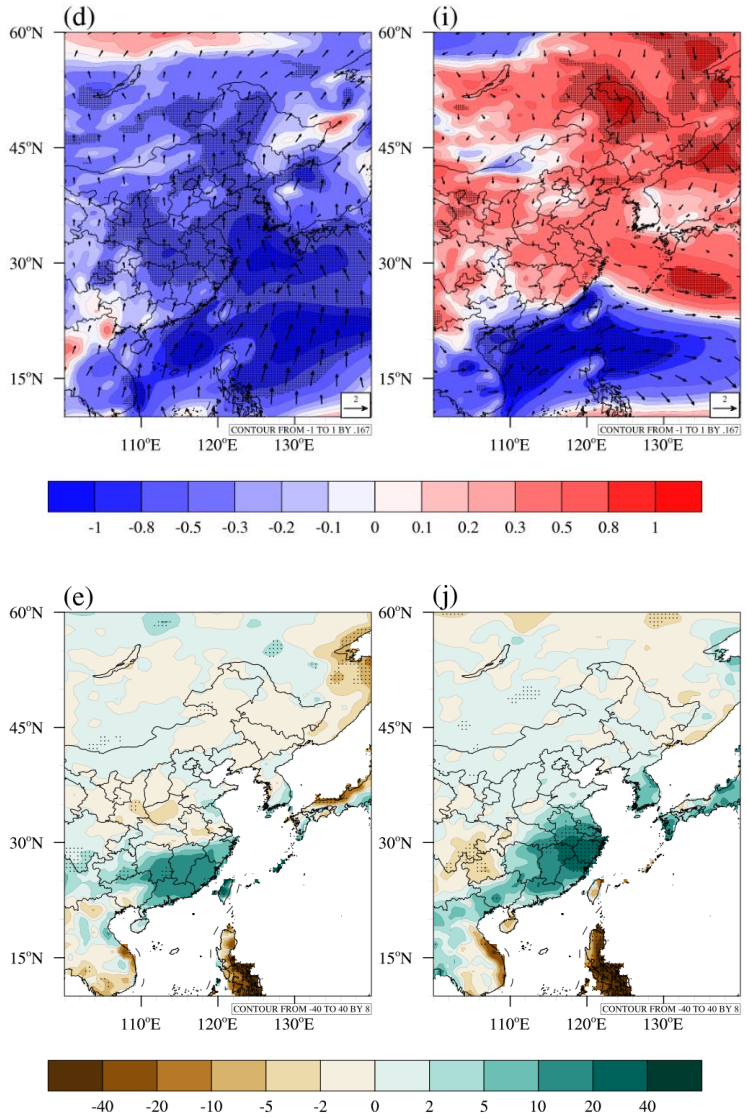

Figure 4: ***(Continued).***

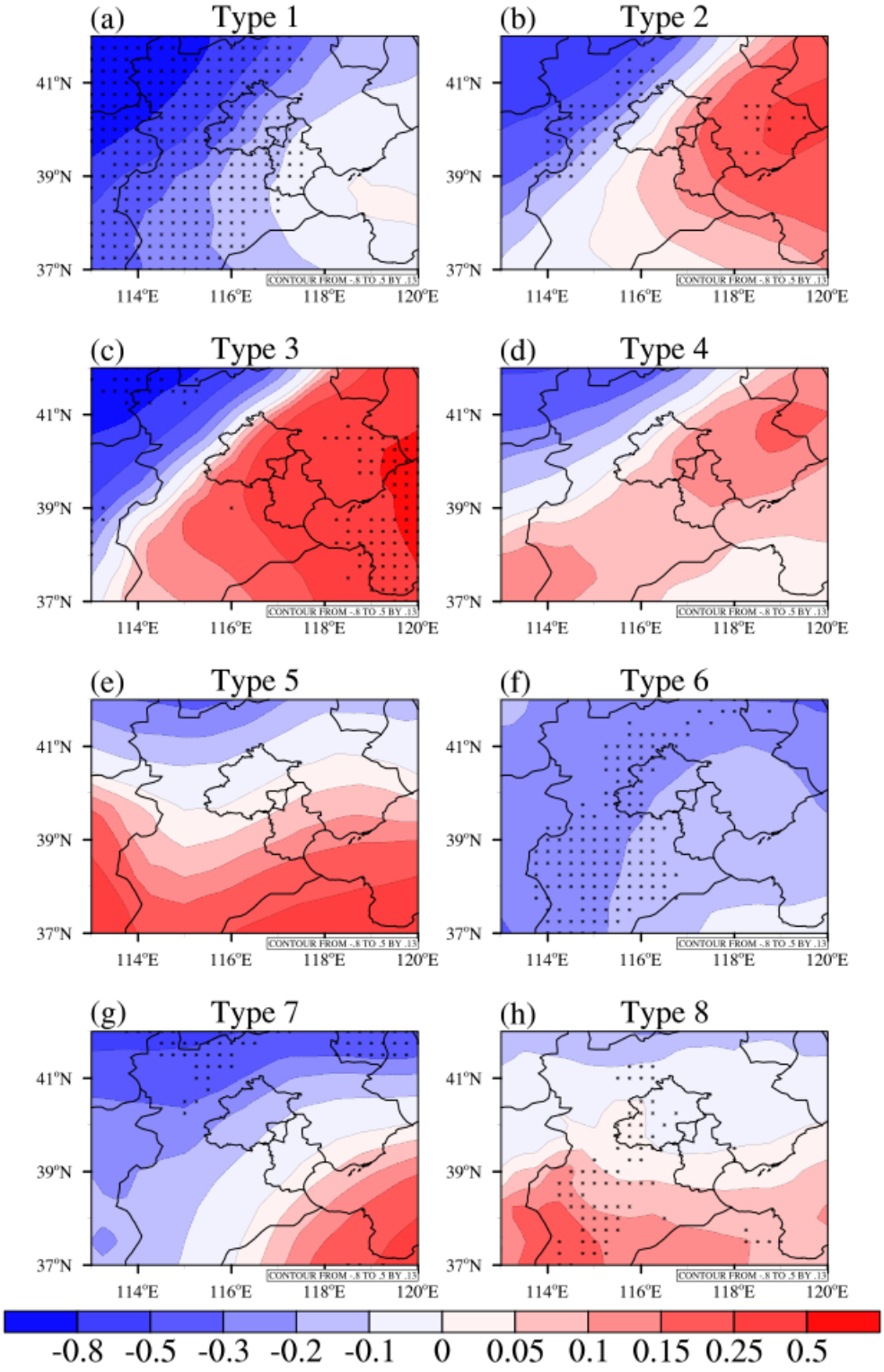

Figure 5: Changes in SLP over JJJ region under eight circulation types in the EP El Niño years relative to the climatological means (unit: hPa). The dots indicate that the differences between more than 60 % of ensemble member pairs have the same sign as the mean differences.

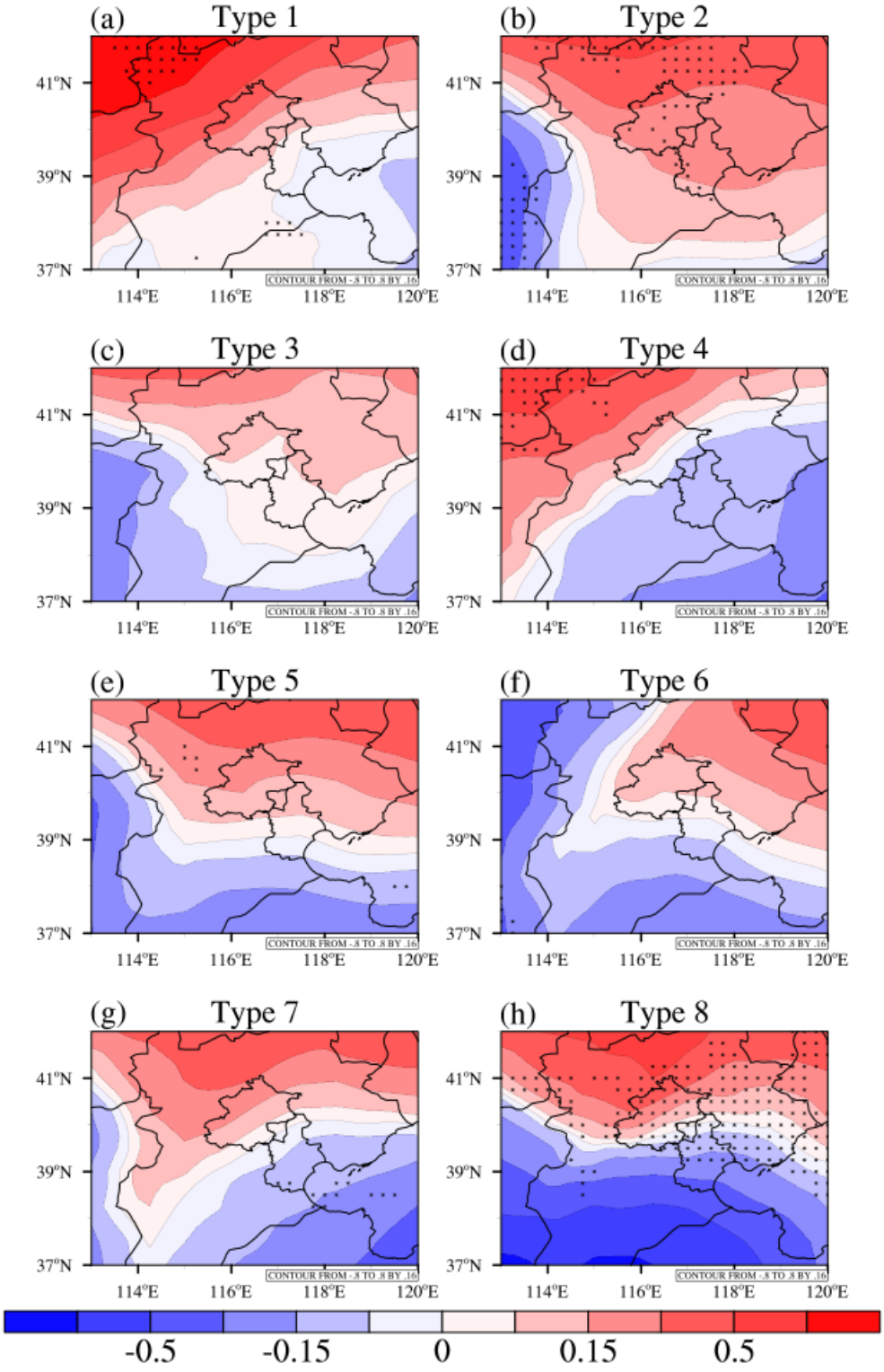

Figure 6: Changes in SLP over JJJ region under eight circulation types in the CP El Niño years relative to the climatological means (unit: hPa). The dots indicate that the differences between more than 60 % of ensemble member pairs have the same sign as the mean differences.

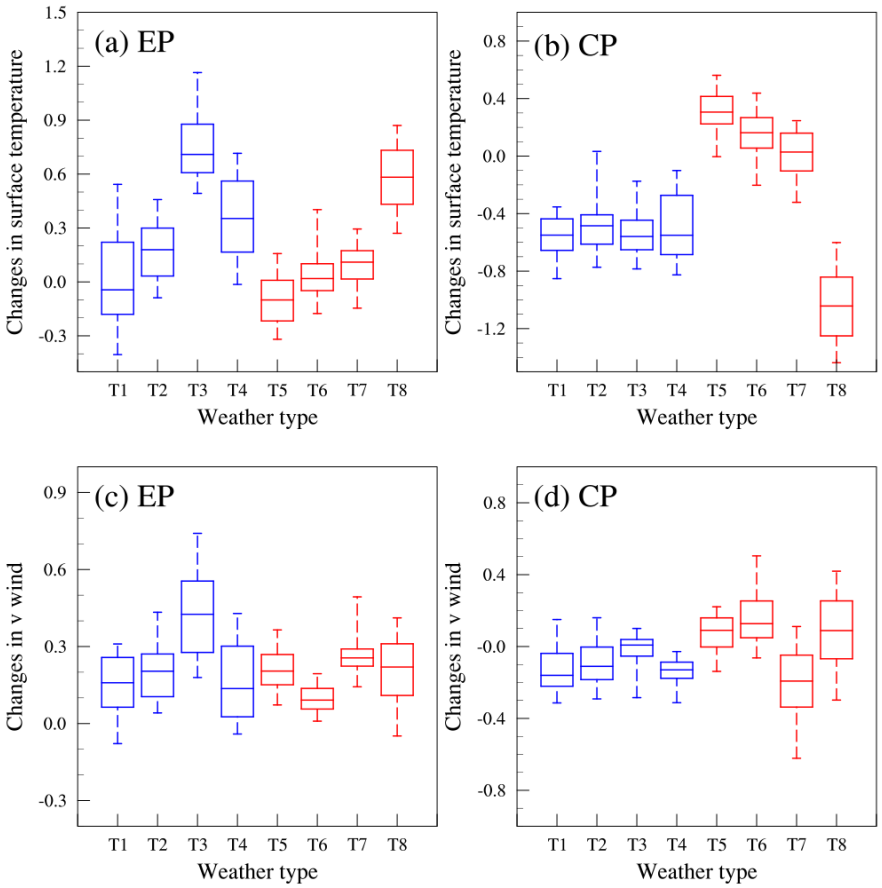

Figure 7: Box-and-whisker plots of anomalies of (a, b) temperature at 2 m (unit: K) and (c, d) meridional wind at 10 m (unit: m s^{-1}) over JJJ region under eight circulation types for different types of El Niño years. The blue and red lines represent the clean and pollution circulation types, respectively. Each box-and-whisker consists of the 5th percentile (the lower point of whisker), 25th quantile (the lower border of box), median (horizontal line in the middle of box), 75th quantile (the upper border of box) and 95th percentile (the upper point of whisker).

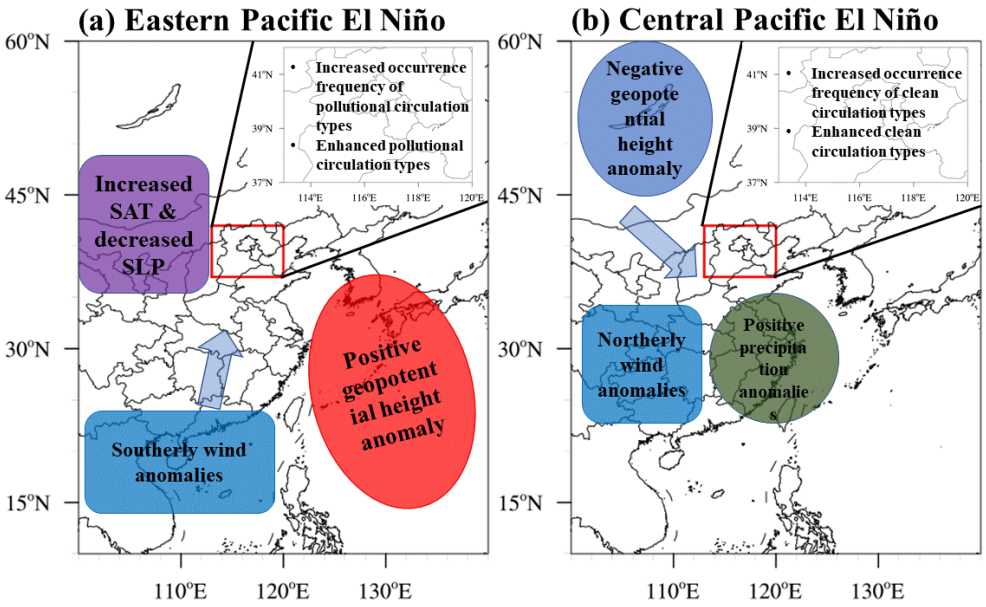

Figure 8: Schematic diagrams showing the physical mechanisms of effects of (a) Eastern Pacific and (b) Central Pacific El Niño on WHD in JJJ region.